Evolution of the East African Rift System from trap-scale to plate-scale rifting

Laurent Michon, Vincent Famin, Xavier Quidelleur

▶ **To cite this version:**

Laurent Michon, Vincent Famin, Xavier Quidelleur. Evolution of the East African Rift System from trap-scale to plate-scale rifting. Earth-Science Reviews, 2022, 231 (2), 10.1016/j.earscirev.2022.104089 . hal-03697015

HAL Id: hal-03697015

https://hal.univ-reunion.fr/hal-03697015

Submitted on 16 Jun 2022

HAL is a multi-disciplinary open access archive for the deposit and dissemination of scientific research documents, whether they are published or not. The documents may come from teaching and research institutions in France or abroad, or from public or private research centers.

L'archive ouverte pluridisciplinaire **HAL**, est destinée au dépôt et à la diffusion de documents scientifiques de niveau recherche, publiés ou non, émanant des établissements d'enseignement et de recherche français ou étrangers, des laboratoires publics ou privés.

Distributed under a Creative Commons Attribution - NonCommercial - NoDerivatives 4.0 International License

Earth-Science Reviews 231 (2022) 104089

Contents lists available at ScienceDirect

Earth-Science Reviews

journal homepage: www.elsevier.com/locate/earscirev

Evolution of the East African Rift System from trap-scale to plate-scale rifting

Laurent Michon [a,b,*], Vincent Famin [a,b], Xavier Quidelleur [c]

[a] Université de La Réunion, Laboratoire GéoSciences Réunion, F-97744 Saint Denis, France
[b] Université Paris Cité, Institut de physique du globe de Paris, CNRS, F-75005 Paris, France
[c] Université Paris-Saclay, CNRS, GEOPS, Orsay 91405, France

ARTICLE INFO

Keywords:
East African Rift System
Volcanism
Extension
LLSVP
Mantle dynamics
Plate dynamics

ABSTRACT

Many continental rifts are subjected to volcanism in tandem with rifting, which has raised a long-standing debate about whether magmatism is the cause or the consequence of plate fragmentation. To re-evaluate this chicken-and-egg question, we took advantage of five decades of research on the East African Rift System (EARS), the largest active continental rift on Earth, to explore the spatial and temporal relationship between rifting and magmatism. By comparing the co-occurrence of tectonics and volcanism since the Eocene with the present-day seismicity, we delimit the EARS as a ~ 5000 km-wide zone of volcano-tectonics made of four branches affecting not only East Africa but also the Mozambique channel and Madagascar. We then developed a quality filtering procedure of published radiometric ages in order to build two independent, robust, and comprehensive age compilations for magmatism and rifting over this extended EARS. Our thorough quality-checked selection of ages reveals that the EARS presents two distinct regimes of volcanism. Since the Upper Eocene, the rift system was affected by (1) pulses of volcanism in 500–1000 km-wide areas, and (2) a discontinuous but remarkably simultaneous volcanic activity, scattered along the four branches of the EARS since 25–27 Ma. Combining this spatio-temporal evolution of volcanism with a critical review of the timing of rifting, we show that the tectonics of the EARS evolves through time from trap-scale to plate-scale rifting. Until the Middle Miocene, extension structures first developed following flood basalt events and plateau uplifts. Then, volcanism resumed synchronously all over the EARS at ca. 12–12.5 Ma, followed by a general extensional deformation. This evolution, which cannot be explained by the sole action of a plume or of tectonics, is therefore interpreted in an intermediate way in which the EARS results from (1) extensive stresses acting on the African lithosphere in the long-lived context of the Gondwana breakup and (2) an overall complex mantle upwelling dynamics arising from the African Large Low Shear Velocity Province (LLSVP). We propose that extension stresses affecting the African lithosphere also modulate the melting of mantle anomalies and/or the collection of magma through the Pan-African belts. This influence explains the synchronous occurrence of many magmatic and tectonic events in the EARS and at the boundaries of the Nubia and Somali plates. Finally, our results suggest that the source of extension stresses affecting the African plate probably evolved from a dominant far-field origin to prevailing variations of gravitational potential energy (GPE) and a diverging basal shear of the Nubia and Somali lithosphere. This change would stem from an increase of the mantle flux in the Middle Miocene, yielding a change in the EARS' dynamics from trap-scale to plate scale rifting.

1. Introduction

The East African Rift System (EARS) is the largest active tectonic structure illustrating the early stage of continental plate fragmentation (e.g., Girdler et al., 1969). It is classically described as made of several extensional basins, two large plateaux, and many volcanic formations of variable spatial extent (Chorowicz, 2005). Indeed, magmatism is widespread and voluminous in the East branch, while it is concentrated in

Abbreviation: AEP, Afar - Ethiopian plateau; EARS, East African Rift System; GNR, Gregory - Nyanza rifts; GPE, Gravitational Potential Energy; LLSVP, Large Low Shear Velocity Province; MER, Main Ethiopian rift; QSA, Quatlamba seismic axis; TBRZ, Turkana broadly rifted zone.

* Corresponding author at: Université de La Réunion, Laboratoire GéoSciences Réunion, F-97744 Saint Denis, France.
E-mail address: laurent.michon@univ-reunion.fr (L. Michon).

https://doi.org/10.1016/j.earscirev.2022.104089
Received 29 November 2021; Received in revised form 7 June 2022; Accepted 8 June 2022
Available online 12 June 2022
0012-8252/© 2022 The Authors. Published by Elsevier B.V. This is an open access article under the CC BY-NC-ND license (http://creativecommons.org/licenses/by-nc-nd/4.0/).

small and scattered volcanic provinces in the West branch and its seaward extension in the Mozambique channel (Fig. 1; Chorowicz, 2005). This striking difference of distribution is responsible for a long-standing debate regarding the link between volcanism and deformation (e.g., Rosendahl, 1987; Bailey, 1992). On the one hand, the EARS may be viewed as entirely (Oxburgh and Turcotte, 1974), or partially (Corti et al., 2003; Armitage et al., 2015) resulting from the deformation of the African lithosphere under far-field stresses, with volcanism being the response of lithospheric deformation as in passive rifts. On the other hand, the coeval occurrence of continental flood basalts and plateau uplift, both prior to extensional basin formation, may arise from one or several mantle plume impingements below the African continental lithosphere as in active rifts (Sengör and Burke, 1978; Hill, 1991; George et al., 1998; Ebinger and Sleep, 1998). Between these two extreme views (plate vs. plume-driven volcano-tectonics; Anderson, 2005, Foulger, 2010), intermediate models involving plume-related buoyancy forces, gravitational potential energy (GPE), basal shear traction, magma-assisted rifting and/or far-field stresses have been proposed to explain the development of the EARS (e.g., Bialas et al., 2010; Kendall and Lithgow-Bertelloni, 2016; Min and Hou, 2018), the coeval openings of the magma-rich eastern and magma-poor western branches (Koptev et al., 2015), or the current plate kinematics (Stamps et al., 2015). All these models remain equally plausible yet undemonstrated as long as the relative influence of plate tectonics and plumes is not evaluated in time (since the initiation of the EARS), and in space (from Afar to the South-West Indian Ridge as defined by kinematic models; e.g., Stamps et al., 2018). In other words, which manifestation, volcanism or lithospheric deformation, occurred first during the EARS evolution over its total extent?

To answer this pivotal question and re-investigate the causes and dynamics of magmatism and extension in the EARS, we (1) clarify the geometry of the rift system, (2) build a comprehensive database of radiometric ages of magmatic activity, taking advantage of decades of published geochronological research, (3) propose a critical review of the published periods of extension from Afar to the Mozambique channel, and (4) interpret the spatio-temporal distribution of the EARS volcanic and tectonic activity in integrating both regional plate and mantle dynamics.

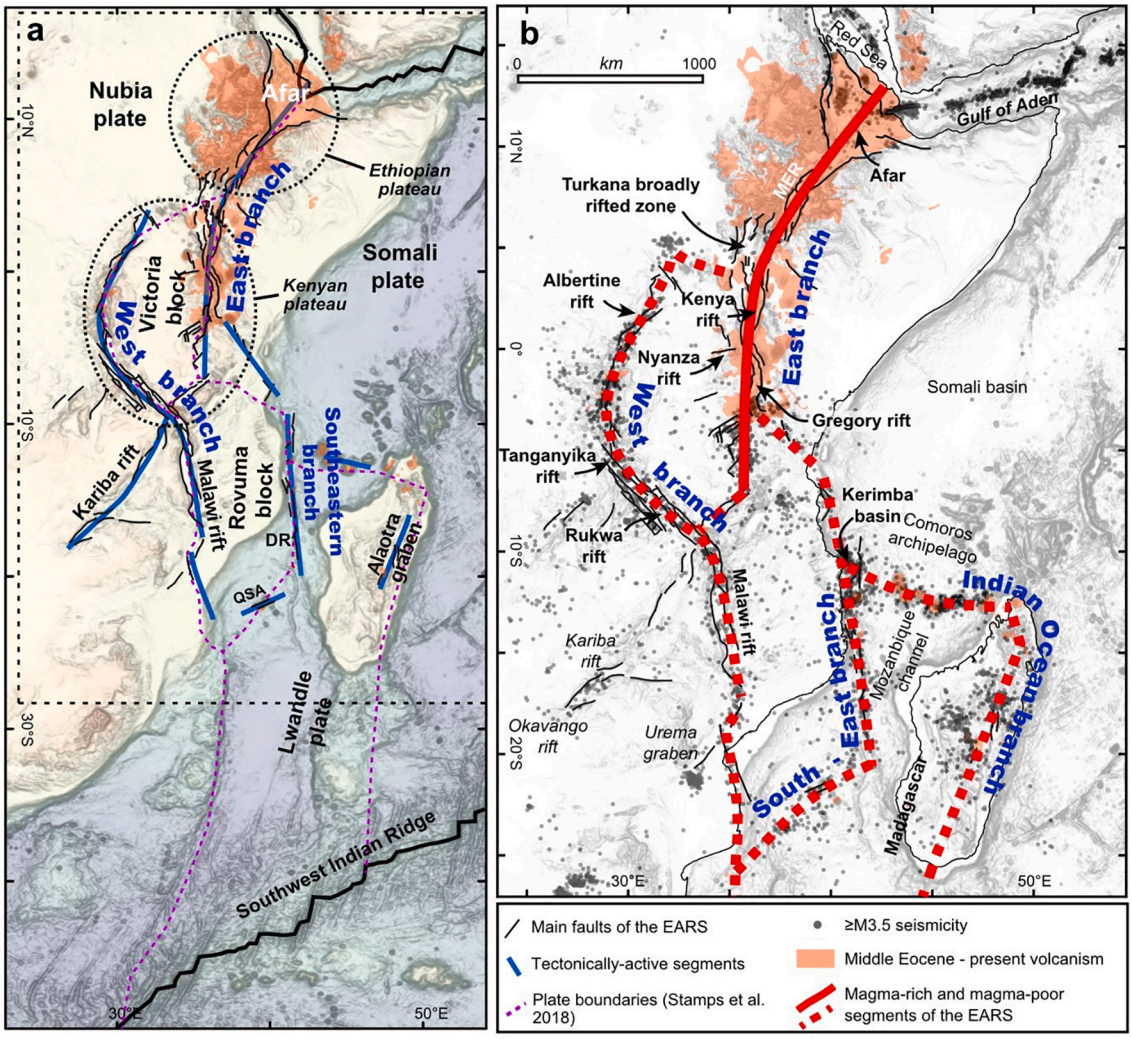

Fig. 1. a) Spatial distribution of Middle Eocene-to-present volcanism and Oligocene-to-present tectonics. The East African Rift System (EARS) was initially defined with two branches (the West and East branches; e.g., Ebinger et al., 1989a). The offshore continuity of the EARS was evidenced by Mougenot et al. (1986) and named the Southeastern branch by Chorowicz (2005). Note that this branch was restricted to the Davie Ridge (DR). QSA: Quatlamba seismic axis. b) Zoom of a), with seismicity added (≥M3.5 from Bertil et al. (2021) for the Mozambique channel and Madagascar and the USGS database for the rest of the EARS). We define the East African Rift System (EARS) as these connected segments of volcanism, faulting and seismicity over a ~ 5000 km-wide zone, including not only the classical East and West branches but also a South-East branch corresponding to the previously defined seaward continuity of the rift system along the Davie ridge (i.e., the Southeastern branch; Chorowicz, 2005) and the Quatlamba seismic axis, and an Indian Ocean branch separating the Lwandle and Somali plates along the Comoros archipelago and Madagascar.

2. Pre-EARS African plate fragmentation

Before the Eocene, the eastern part of the African plate experienced several periods of extension that contributed to the fragmentation of the Gondwana (e.g., Macgregor, 2018, for a review). First, the poly-phased Karoo rifting event dated from the Middle Permian to the Middle Jurassic led to the development of a ~ 3000 km-long system of grabens parallel to the east continental margin of the current African continent (Fig. 2a; Castaing, 1991; Catuneanu et al., 2005). It was followed by the Late Jurassic - Early Cretaceous southward drift of Madagascar along the Davie ridge main transfer zone, which opened the Mozambique and Somali basins (Coffin and Rabinowitz, 1987; Cochran, 1988), and by the early Cretaceous extension in Kenya and South Sudan, which opened the NW-SE-striking Anza, Muglad, Blue Nile, and Melut grabens (Guiraud and Maurin, 1992; Ebinger et al., 2000) and the Rukwa rift between the Tanganyika and Zambia cratons (Fig. 2b; Roberts et al., 2010). Finally, during the Upper Cretaceous and Early Paleogene, extension resumed in the Anza, Muglad and Melut grabens until a regional inversion in the Eocene (Bosworth, 1992; Guiraud and Bosworth, 1997). The Eocene period corresponds to the onset of the first volcanic activity attributed to the EARS, in the Turkana area around 45 Ma, between the Muglad and Anza grabens (Ebinger et al., 1993a; George et al., 1998). Thus, in a similar fashion to Macgregor (2015), we consider the Middle Eocene magmatic activity as the starting point of the evolution of the EARS, even if a younger age (Late Eocene) has been proposed by Morley et al. (1999a) from sedimentary infill in the Turkana Broadly Rifted Zone. Interestingly, these Middle and Late Eocene ages correspond to the initiation of the incipient separation (Hempton, 1987) and effective extension between Africa and Arabia (Bosworth et al., 2005; Bellahsen et al., 2006), suggesting that a broader plate reorganisation started at this time in the framework of Africa-Eurasia convergence (Hempton, 1987; Jolivet and Faccenna, 2000).

3. Geometry of the East African Rift System

There is no consensus over the extent of the EARS. Mostly based on the distribution of grabens, the EARS is often defined as a tectonic structure limited to the African continental lithosphere, made of two branches, East and West, and an incipient South-West continuity along the Okavango rift zone (Fig. 1a; Ebinger et al., 1989a, 1993b; Modisi et al., 2000; Kinabo et al., 2007; Pastier et al., 2017). However, marine geophysics suggests that the EARS not only affects the African continent but continues in the Mozambique channel along the Davie Ridge (Mougenot et al., 1986; Franke et al., 2015), forming a Southeastern branch (Fig. 1a; Chorowicz, 2005). Recent offshore surveys have evidenced a southward continuity of this segment along the Quatlamba seismic axis (Courgeon et al., 2016, 2017; Deville et al., 2018). Furthermore, the development of N-S trending grabens in Madagascar since the Pliocene (like the Alaotra graben; Piqué et al., 1999; Kusky et al., 2010) could represent the easternmost manifestation of the plate

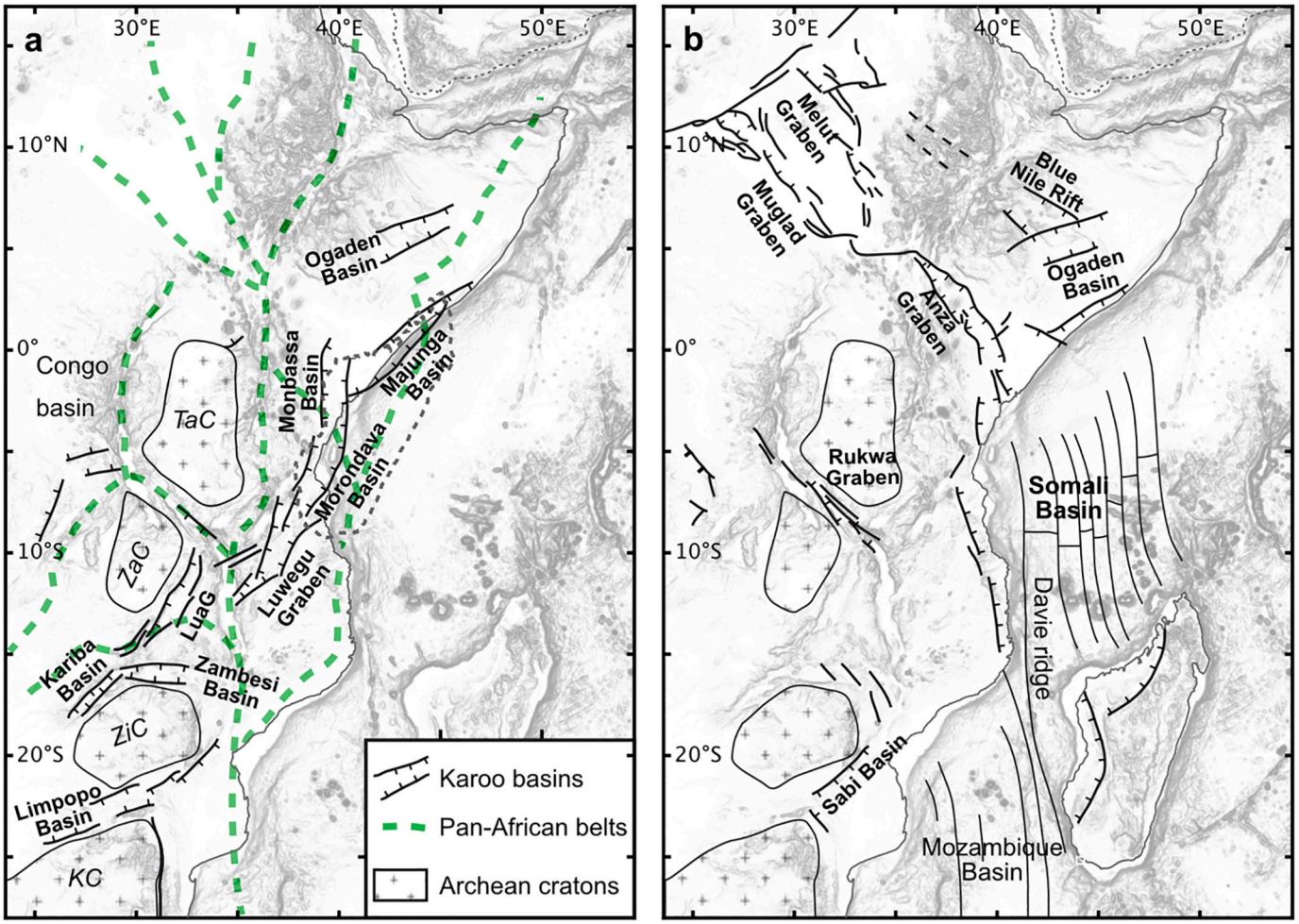

Fig. 2. Grabens and basins formed during (a) the Middle Permian – Middle Jurassic Karoo and (b) Lower Cretaceous rifting events. Paleoposition of Madagascar in thick dashed line from Phethean et al. (2016). The Somali basin opened during the Latest Jurassic – Lower Cretaceous southward drift of Madagascar (Coffin and Rabinowitz, 1987; Cochran, 1988). LuaG: Luanga graben. TaC, KC, ZaC and ZiC account for the Tanzanian, Kaapvaal, Zambia, Zimbabwe cratons, respectively. Pan-African orogenic belts after Shackleton (1996), Begg et al. (2009) and Vérard (2021).

extension (Fig. 1a; Kusky et al., 2010; Michon, 2016). In addition, kinematic models suggest that the EARS spreads out from Afar to the Southwest Indian Ridge along segments that delimit lithospheric blocks/plates between the Somali and Nubia plates (Fig. 1a; Hartnady, 1990; Jestin et al., 1994; Calais et al., 2006; Horner-Johnson et al., 2007).

In the present study, we use the spatial coexistence of Tertiary volcanic activity, Oligocene-to-present tectonics, and seismicity, as criteria to delineate the segments of long-term plate deformation and volcanism of the EARS. The occurrence of volcanism, which is mostly mafic in the EARS (e.g., Furman, 2007), evidences mantle melting due to either rift-induced lithospheric thinning and/or mantle anomaly impingement, whereas the past tectonics and current seismicity give insights into the past and active lithospheric deformation. Compiled in Fig. 1b, these criteria confirm the geometry of the East and West branches and the occurrence of an offshore continuity along the northern part of the Davie ridge, which was named the Southeastern branch by Chorowicz (2005). Recent offshore data reveal (1) that a late Cenozoic volcanism and deformation occurred along the southern part of the Davie ridge (Courgeon et al., 2018) and (2) that this segment is connected to the Quatlamba axis (Deville et al., 2018) and the Natal province, where it merges with the N-S trending West branch (Fig. 1b). Moreover, the offshore continuity may also extend toward the Comoros archipelago, formerly interpreted as a hotspot track (Emerick and Duncan, 1982; Class et al., 1998). However, the alignment of the Comoros is not consistent with the absolute motions of the Somali or Lwandle plates (Wang et al., 2018). Furthermore, we recently showed that the coexistence of en-échelon Quaternary volcanic lineaments in the archipelago, of focused seismic activity with dominant strike-slip focal mechanisms (Bertil and Regnoult, 1998; Lemoine et al., 2020), and of prominent strike slip faulting affecting the islands since at least 1 Ma, all indicate that the Comoros archipelago is a right-lateral boundary between the Lwandle and Somali plates rather than a hotspot track (Famin et al., 2020). Such a right-lateral displacement between the Somali and Lwandle plates along the Comoros archipelago is consistent with GPS data (e.g., Stamps et al., 2018). The coexistence of volcanism, N-S grabens and seismicity in Madagascar suggests that the plate boundary forms a 90° sharp bend toward the south. Thus, we propose that the Comoros and Madagascar segments form a fourth branch in the EARS,

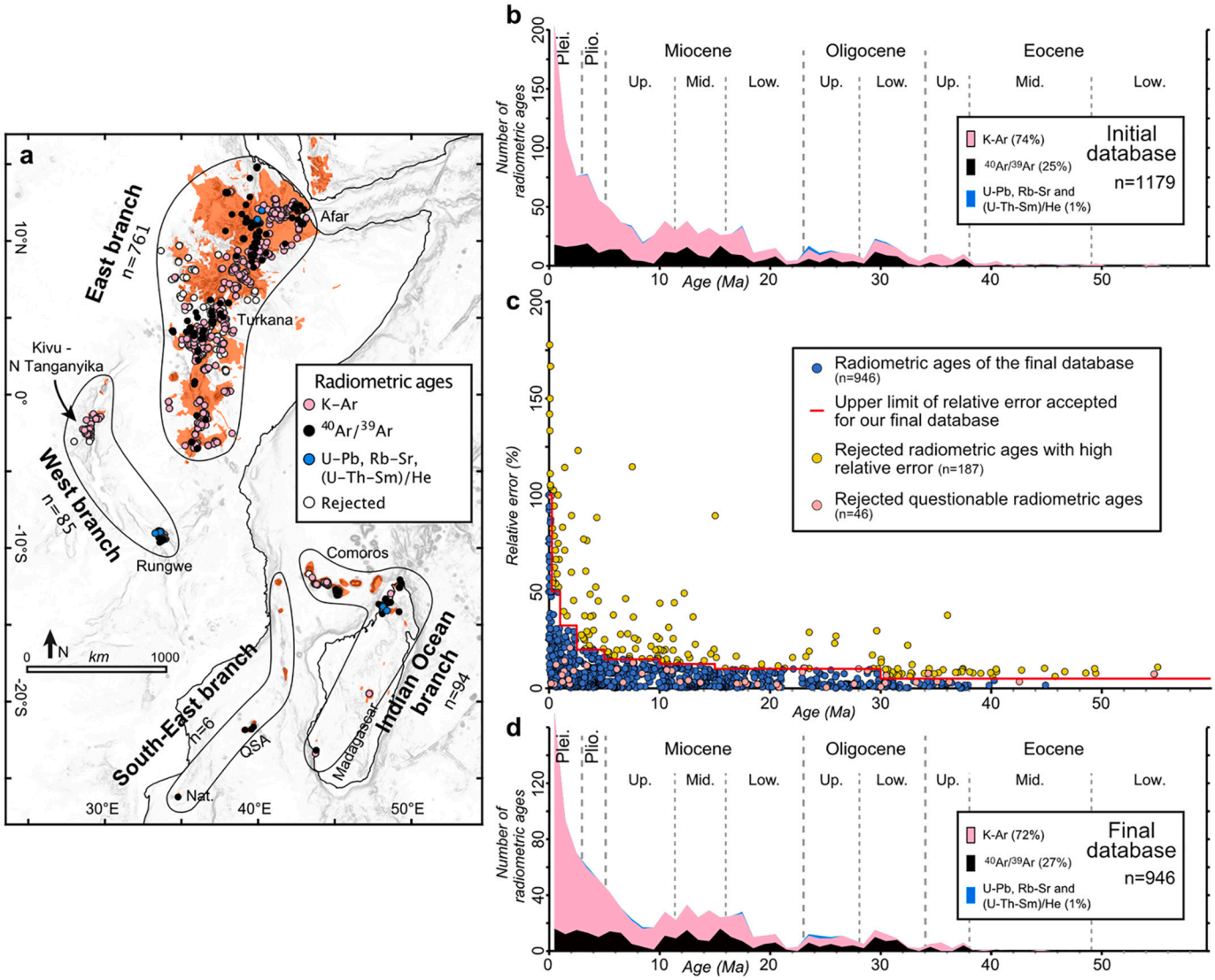

Fig. 3. a) Spatial repartition of the radiometric ages of volcanism integrated in the database according to the dating technique used (see Supplementary Table S1 for the data and Supplementary Material for the references). b) Temporal distribution of all the radiometric ages available in the 81 publications constituting our database whatever their reliability. c) Filtering of the radiometric ages considering their relative error for a 2σ uncertainty and their reliability mainly due to the level of weathering of the samples. d) Temporal distribution of all the remaining radiometric ages after applying the filtering procedure described in the text (Supplementary Table S3).

which we call the Indian Ocean branch. The concentration of magmatism, faults and earthquakes along the volcano-tectonic corridors of the Comoros archipelago, the Davie ridge, Madagascar and the Quatlamba axis, suggests that the South-East and Indian Ocean branches are likely not a diffuse deforming zone as proposed by Kusky et al. (2010) and Stamps et al. (2018, 2021), but rather delineates the Lwandle plate.

4. Material and methods

4.1. Dating volcanism

To refine the history of volcanic activity along the EARS, we compiled the published georeferenced radiometric ages available for Tertiary magmatic rocks over the East, West and South-East branches (Fig. 3a). Instead of integrating all the published ages since the pioneer work of Evernden et al. (1957), we applied the following procedure to ensure the robustness of the database. (1) Radiometric studies older than 1980 were not considered because dating methods of young mafic igneous rocks were still under development at that time. We made three exceptions to this rule for Grommé et al. (1970), Fairhead et al. (1972) and Hajash and Armstrong (1972), because they corroborated their radiometric ages with paleomagnetic polarities. The initial database was thus composed of 1179 radiometric ages available in 81 publications (Fig. 3a, b; Supplementary Table S1; all the references are in Supplementary Material). (2) Age uncertainties were homogenized to the 2σ level. Data presenting high 2 sigma uncertainties with respect to their age were rejected with the following relative uncertainty cut-offs: >5%, >10%, >12.5%, >15%, >20%, >30%, >50%, and > 100% for ages >30 Ma, between >15–30 Ma, between >10–15 Ma, between >5–10 Ma, between >2.5–5 Ma, between >1–2.5 Ma, between 0.25 and 1 Ma and < 0.25 Ma, respectively (Fig. 3c). This step eliminated 16.1% of the initial database. (3) Forty-five radiometric ages (i) described as in contradiction with stratigraphic successions, (ii) obtained on samples presenting evidence of significant alteration, or (iii) poorly constrained from their dating method (e.g., absence of plateau for the $^{40}Ar/^{39}Ar$ approach) were not integrated in the final database. (4) All the radiometric ages using the ^{40}K decay were recalculated with the same decay constant, and ages determined with the $^{40}Ar/^{39}Ar$ method were recalculated with the same standard (Fish Canyon Tuff sanidine at 28.201 Ma; Kuiper et al., 2008). This entire filtering procedure resulted in the rejection of 233 radiometric ages (20% of the initial database; Supplementary Table S2), with the advantage of minimizing the inevitable oversampling of the most studied volcanic provinces and periods.

Our final database is made of 946 radiometric ages (761, 85, 6 and 94 data for the East, West, South-East and Indian Ocean branches, respectively; Fig. 3a) in which K-Ar, $^{40}Ar/^{39}Ar$ and U-Pb, Rb-Sr or (U-Th-Sm)/He ages account for 72%, 27%, and 1% of the database, respectively (Fig. 3d; Supplementary Table S3). This comprehensive database provides a useful representation of volcanic periods, but it must be kept in mind that non-systematic sampling may result in temporal and spatial biases that cannot be avoided. Furthermore, it must be stressed that the abundance or scarcity of radiometric ages for a given volcanic period

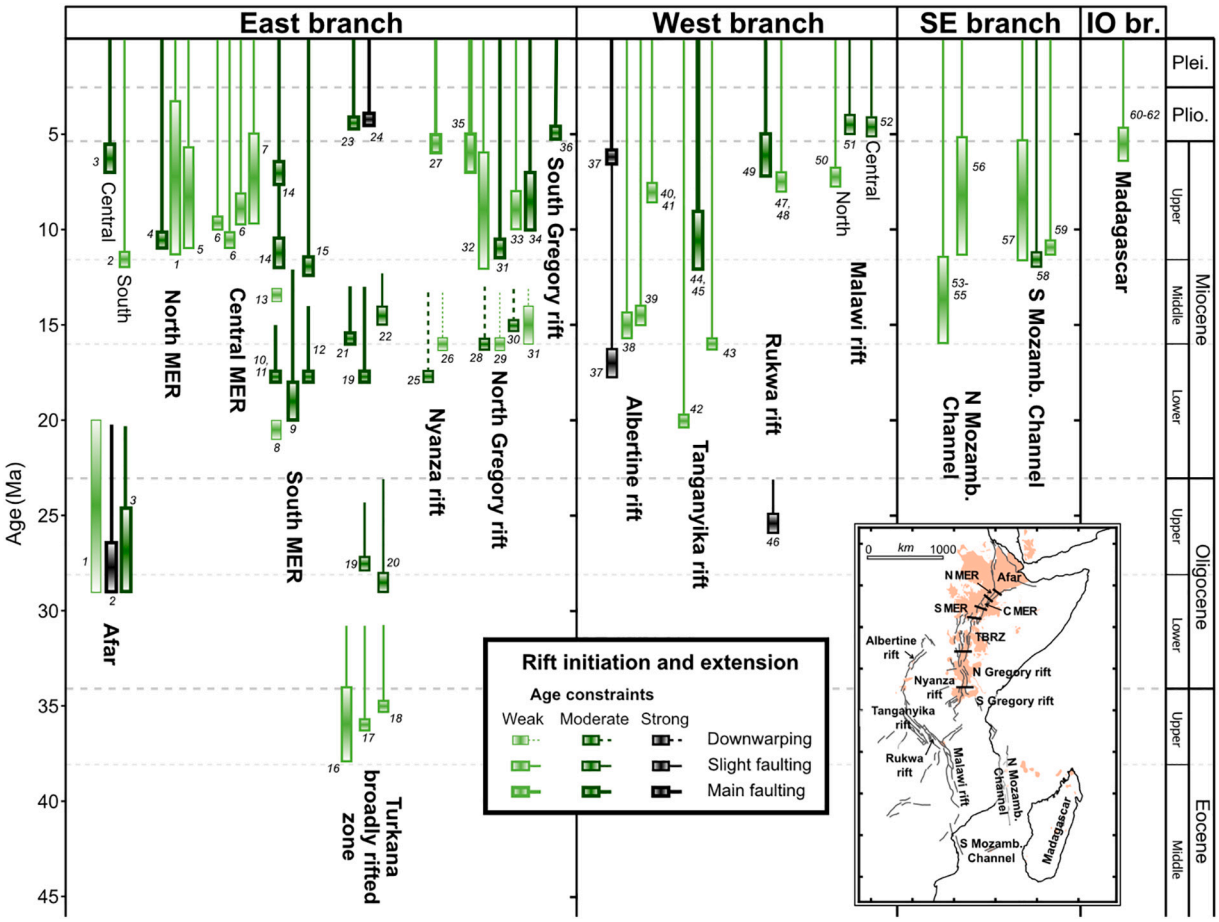

Fig. 4. Synthesis of the published documented periods of rifting in the different branches of the EARS. The symbols colour accounts for weakly to strongly constrained periods of extension. See text for the quality determination methodology. IO br.: Indian Ocean branch; MER: Main Ethiopian Rift; TBRZ: Turkana broadly rifted zone. Boxes and lines account for the age of rift initiation and the duration of extension, respectively. The size of each box takes into account the time range of rift initiation determined from age constraints (see supplementary Table S4 for age constraints). Numbers refer to the publications compiled in Supplementary Table S4 and listed in Supplementary Material.

does not provide any insight regarding the volume of emitted magma, but only indicates that the area experienced volcanism at that time.

4.2. Dating rifting initiation

To assess the potential genetic link between lithospheric deformation and magmatism, we synthesised the documented periods of extension that affected the EARS since the Middle Eocene, from Afar to the Mozambique channel (Fig. 4; Supplementary Table S4; all the references are in Supplementary Material). We compiled 63 publications in which the periods of rifting have been dated from radiometric ages of pre-, syn- and/or post-rift volcanic products (e.g., McDougall and Watkins, 1988; Behrensmeyer et al., 2002; Roberts et al., 2012b; Stab et al., 2016), from apatite fission track or (U-Th-Sm)/He thermochronology (Spiegel et al., 2007; Pik et al., 2008; Philippon et al., 2014; Torres Acosta et al., 2015; Balestrieri et al., 2016; Boone et al., 2018), from biostratigraphy (e.g., Kent et al., 1971; Suwa et al., 1991; Bromage et al., 1995; Simon et al., 2017; Courgeon et al., 2018), or, in areas lacking any volcanic or paleontological markers, from indirect methods such as seismic reflection, orbital stratigraphy and rates of sediment accumulation or rift propagation (e.g., Morley, 1988; Mougenot et al., 1989; Cohen et al., 1993; Franke et al., 2015; McCartney and Scholz, 2016; Ponte et al., 2019).

For each publication, we made a critical review of the criteria used to accurately date the rift initiation and the periods of extension and therefore rated the proposed ages of extension as strongly, moderately and weakly constrained (Fig. 4; published periods of extension in Supplementary Table S4). Rifting events dated with radiometric dating of volcanic formations were rated as follows. The robustness of radiometric ages that were used to date rifting events was first checked considering the approach described in section 4.1. We therefore did not consider in most cases the periods of rifting dated with ages that we rejected, but exceptionally kept rifting events dated with radiometric data obtained before 1980, when these data were the only available to date extension. The latter were rated as weakly constrained. For extension initiation dated using pre- and syn-rift lava units whose radiometric ages were considered as reliable, we computed an average age from the proposed pre- and syn-rift dates. Ages of rift initiation were then considered as strongly, moderately and weakly constrained when the time span between the pre- and syn-rift dates accounts for $<10\%$, between 10 and 30% and $>30\%$ of the average age, respectively (see the example of the Afar segment in Supplementary Table S4; Ukstins et al., 2002; Wolfenden et al., 2005; Stab et al., 2016). Rifting events dated with pre- and post-rift formations (e.g., McDougall and Watkins, 1988; Boschetto et al., 1992) were considered as moderately constrained since the pre-rift unit provided only a maximum age for rift initiation. Several periods of rifting have been dated from the thickening of a volcanic unit in the grabens (e.g., Wolfenden et al., 2005). As the thickening of the volcanic formation only indicates the existence of a topographic depression, it provides a minimum age of rift initiation. Rift initiations dated with syn-rift formations were consequently considered as weakly constrained. Yet, the occurrence of syn-tectonic units (Wolfenden et al., 2004) or several syn-rift volcanic units interstratified in sediments (e.g., Boschetto et al., 1992; McDougall and Brown, 2008) were considered as reliable features to accurately date periods of extension and were thus rated as moderately constrained. Finally, rifting events dated from radiometric ages of volcanic intrusions (e.g., Bonini et al., 2005) or of off-rift volcanic vents (e.g., Ebinger et al., 2000; Ebinger et al., 1993b) were rated as weakly constrained because off-rift volcanism has been shown to be primarily controlled by topography effects rather than regional extension stresses (Maccaferri et al., 2014).

The exhumation of rift shoulders related to major extension events have been dated by apatite fission track analysis or (U-Th)/He thermochronology (Spiegel et al., 2007; Pik et al., 2008; Philippon et al., 2014; Torres Acosta et al., 2015; Balestrieri et al., 2016; Boone et al., 2018). In these different studies, the onset of rapid exhumation determined from thermal models was considered as indicative of rift initiation. We rated these ages as moderately constrained except when the results were contradicted by more recent thermochronometry data and radiometric ages. They were consequently lowered to weakly constrained (e.g., Spiegel et al., 2007 for the Northern Gregory rift).

In areas lacking volcanic rocks to date the periods of extension, molluscs, vertebrates, pollens, spores, nannofossils or planktonic foraminifers embedded in the syn-rift sediments have tentatively been used to determine the age of the rifting events. The dating accuracy depends on the specificities of the fossil assemblages. We therefore rated as weakly constrained the periods of rifting determined from a fauna poorly characteristic of a given period, as in Madagascar for the Pliocene extension (Bésairie, 1960; Supplementary Table S4). In contrast, fauna assemblages representative of a specific period were considered as moderately to strongly constrained depending on the existence of additional methods to date the rifting events (e.g., E.M. Roberts et al., 2012b; Simon et al., 2017).

Finally, the graben structure of several segments of the EARS have been imaged from reflection seismology and dated from the stratigraphy deduced in deep drill holes, the estimate or determination of Quaternary or current sedimentation rates, dated intercalated lava units, or estimates of rift lateral propagation. In general, we rated as weakly and moderately constrained the rifting periods dated from the extrapolation of current and Quaternary accumulation rates, respectively. The ages of periods of rifting dated by the stratigraphy recorded in deep wells were considered as weakly constrained since the time span between the identified horizon frequently exceeds several million years (duration of 4–8 Myrs of the epochs of the Eocene, Oligocene and Miocene), making estimation of the initiation of fault activity imprecise. Finally, the determination of the age of rift initiation from estimates of rift southward propagation (e.g., the Lacerda graben in the Mozambique channel; Franke et al., 2015) is rated as weakly constrained because more recent results indicate that rifting initiated at the Middle-Late Miocene transition in the southern Mozambique channel (Deville et al., 2018).

5. Results

5.1. Spatio-temporal distribution of volcanism

At first glance, the compilation confirms that the East branch underwent an onset of volcanism in the Middle Eocene (Fig. 5a), ~20 Ma earlier than the West, South-East and Indian Ocean branches (Fig. 5b, c and d). It also shows a simultaneous initiation of magmatic activity, dated with several radiometric methods, since the Upper Oligocene in both West and Indian Ocean branches. This early coeval activity is hardly compatible with the progressive outward influence of the Afar plume proposed by Ebinger and Sleep (1998).

Thus, we subdivided the EARS into several volcanic provinces based on their structural specificities (Fig. 6) to evaluate potential differences in the evolution of each branch, for instance due to the influence of one or several mantle plumes, as discussed by Emerick and Duncan (1982), Ebinger and Sleep (1998), and George et al. (1998). For the East branch, we took into account the topographic low made by the Turkana broadly rifted zone (TBRZ) between the Ethiopian and Kenyan plateaux (Fig. 1b; George et al., 1998) and its precursory extension (Macgregor, 2015; Morley et al., 1992) to distinguish it as a separate volcanic province located between those of the Afar - Ethiopian plateau (AEP) in the north, and the Gregory - Nyanza rifts (GNR) in the south (Fig. 6). The West branch was subdivided into two distinct volcanic provinces, Kivu - N Tanganyika and Rungwe, based on the gap of volcanism between them. The South-East branch is the least dated of the EARS with only six ages. We therefore prefer to consider it as a single volcanic province instead of two provinces characterized by three dates each, i.e., the Natal and Quatlamba seismic axis. Lastly, the Indian Ocean branch has been subdivided into two volcanic provinces: (1) the Comoros archipelago, the northern tip of Madagascar, and the submarine edifices in-between, and (2) the central and southern parts of Madagascar. Following our revised

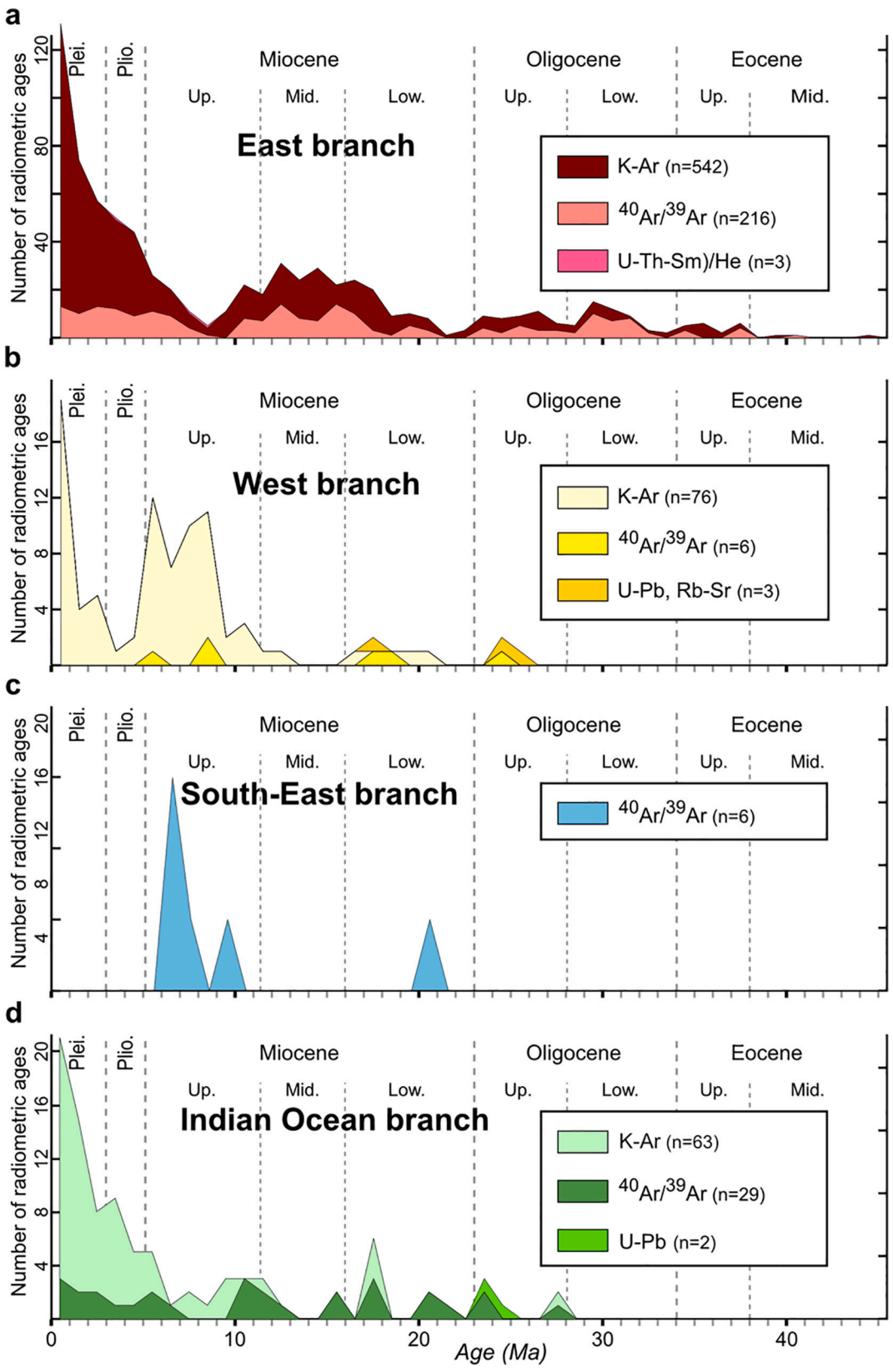

Fig. 5. Temporal distribution of radiometric ages since the Middle Eocene for the East branch (a), for the West branch (b), and for the South-East branch (c). Distinction is made between radiometric methods to allow their intercomparison. Note that this figure does not provide any information on magma volume but solely the number of radiometric ages. It therefore highlights the periods with the highest constraints on the age of volcanic activity (i.e., periods with several dated samples and/or with several methods used to date the activity).

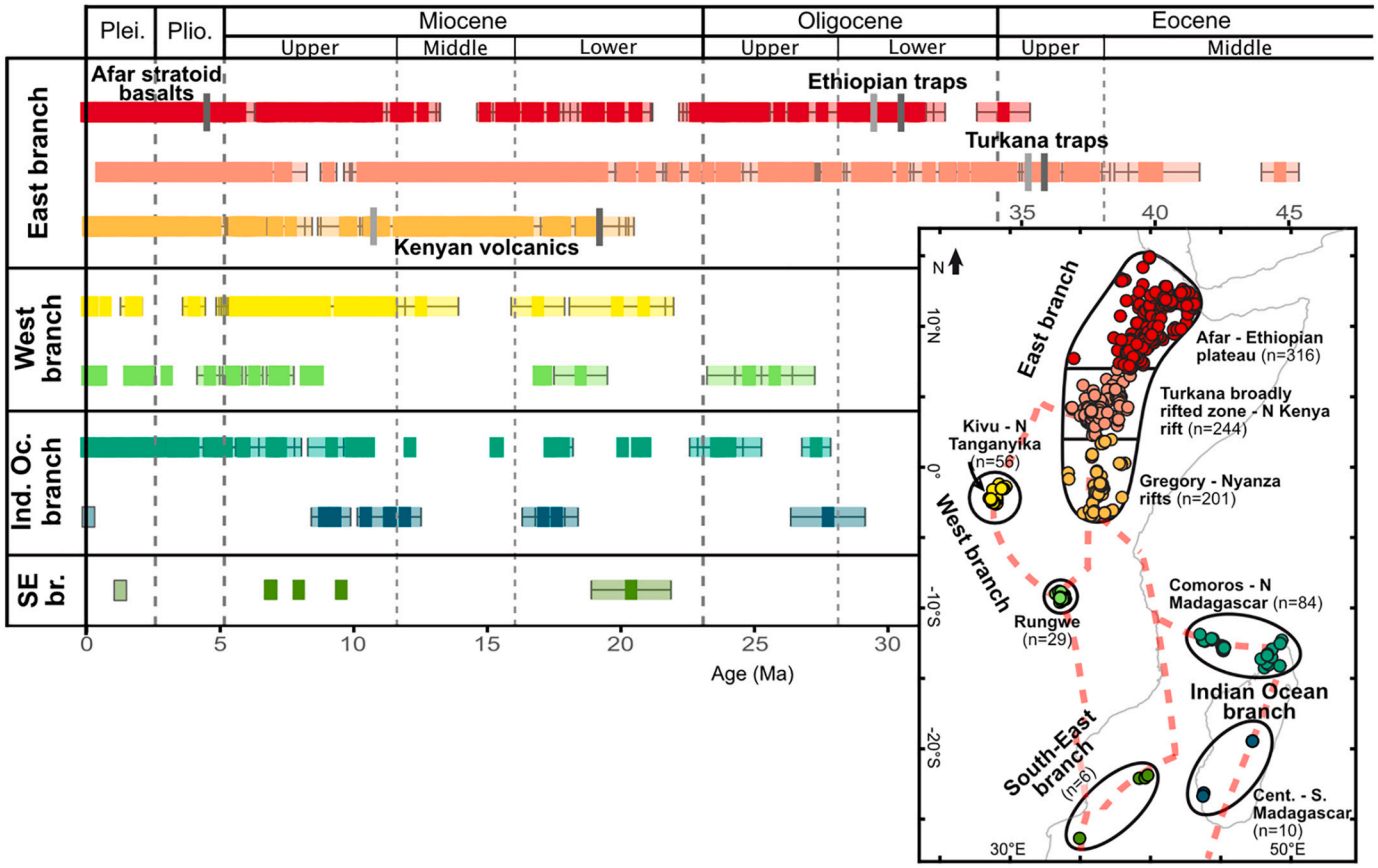

Fig. 6. Temporal distribution of volcanism in the EARS, subdivided into volcanic provinces represented in the inset map. For each province, bright colours account for periods of volcanism dated by radiometric ages, while light colour bars integrate the radiometric uncertainties (error bars on isotopic ages are 2σ). The light blue and light green boxes indicate the occurrence of a Pleistocene volcanic activity along the Central – South Madagascar province (Rufer et al., 2014) and the South-East branch (Courgeon et al., 2017), respectively. Dark and light grey vertical lines account for the commencement and termination of the trap events, respectively. Red dotted lines in the inset map represent the limits of continental blocks defined in Fig. 1. See Supplementary Fig. S1 to visualize the error bars of individual data in each province. (For interpretation of the references to colour in this figure legend, the reader is referred to the web version of this article.)

geometry of the EARS, these two provinces developed along the E-W and N-S boundaries between the Lwandle and Somali plates (Fig. 6).

Our subdivision of the EARS' branches into volcanic provinces may be applied to the database of radiometric ages in order to explore the temporal evolution of magmatic activity (Fig. 6). In this temporal evolution, some features were already noticed by previous studies. For instance, the volcanic activity of the East branch was almost exclusively restricted to the TBRZ during the Eocene, consisting first in a few initial eruptions around 40–45 Ma and followed by a bimodal emission of flood basalts and rhyolitic ignimbrites around 35–37 Ma that emitted around 30–100 $\times$ 10^3 km^3 of lava (Ebinger et al., 1993a, 2000; McDougall and Brown, 2009; McDougall and Watkins, 2006). At that time, a very limited activity was found in the AEP volcanic province (George et al., 1998). The main magmatic event of the East branch occurred around 30 Ma with the emplacement of the Ethiopian traps in the AEP province. This event emitted around 300 $\times$ 10^3 km^3 (Mohr, 1983; Ebinger et al., 1993a) in a short time span (Hofmann et al., 1997). Our compilation shows that the TBRZ and AEP provinces experienced a relatively different discontinuous activity until half of the Lower Miocene, as a volume of around 100 $\times$ 10^3 km^3 of flood basalts and rhyolitic ignimbrites (the Kenyan volcanics) was emitted in both the TBRZ and the Gregory - Nyanza volcanic province at 11–19 Ma (Williams, 1982; Itaya and Sawada, 1987; Boschetto et al., 1992; George et al., 1998; McDougall and Feibel, 1999; Ebinger et al., 1993a, 2000; Behrensmeyer et al., 2002), while the AEP province became almost quiescent (Fig. 6). The magmas emitted during these periods of intense volcanic activity display tholeiitic to alkaline compositions (e.g., Fitch et al., 1985; Hart et al., 1989; Kampunzu and Mohr, 1991; Kieffer et al., 2004; Furman, 2007).

More remarkably, our subdivision also reveals that the Indian Ocean and West branches present a nearly similar temporal evolution of magmatism. They experienced an Upper Oligocene and Lower Miocene discontinuous activity, a quiescence over most of the Middle Miocene, followed by a coeval resumption of activity around 12–12.5 Ma in 3 of the 4 volcanic provinces, and finally a generalised volcanism from the Upper Miocene onward in all the provinces (Fig. 6). It is worth noting that the Central - South Madagascar volcanic province is still active despite a lack of radiometric ages, as indicated by the Pleistocene-Holocene Itasy and Vakinankaratra volcanic fields (Fig. 6; Rufer et al., 2014; Melluso et al., 2018). Furthermore, the evolution of the Indian Ocean and West branches is remarkably similar to that of the submarine edifices of the South-East branch that displayed an Upper Oligocene – Lower Miocene main building period, followed by an Upper Miocene – Pleistocene discontinuous activity (Fig. 6; Courgeon et al., 2017; O'Connor et al., 2019; Berthod et al., 2022). Magmas emitted in the West, Indian Ocean and South-East branches not only show a similar timing, but also share identical chemical affinities of the silica-saturated, silica-undersaturated alkaline, and melilitic-carbonatitic suites (e.g., Kampunzu and Mohr, 1991; Späth et al., 1996; Rudnick et al., 1993; Furman, 2007; Pelleter et al., 2014; Mazzeo et al., 2021; Berthod et al., 2022).

A key result arising from our compilation of radiometric ages is that the common evolution described above is not limited to the West, South-East and Indian Ocean branches, but is also observed in the distant AEP

province (Fig. 7). These different provinces are all characterized by an Upper Oligocene / Lower Miocene discontinuous volcanism with coeval peaks, a significant hiatus during most of the Middle Miocene (12.5–15 Ma) and a volcanic renewal from 12 to 12.5 Ma on (Fig. 7). Interestingly, the volcanic episode recorded between around 17–18.5 Ma in all the provinces initiated at the same time as the Kenyan volcanics in the TBRZ and Nyanza rift (Fitch et al., 1985; Drake et al., 1988).

The TBRZ and GNR provinces share a magmatic evolution that differs from the other provinces. They underwent an intense volcanic activity at 11–19 Ma and present a hiatus between 9.1 and 7.4 Ma, confirmed in the field by the lack of volcanic deposits in the sediments and by an angular unconformity (Sawada et al., 1987; Tatsumi and Kimura, 1991; McDougall and Feibel, 1999).

Importantly, we can rule out a possible effect of our filtering of age data in the results described above because the latter still stand when integrating all the ages of the initial pre-filtering database (Fig. 3b; Supplementary Fig. S1b).

5.2. Timing of extension

Our compilation of the periods of extension along the entire EARS reveals that several ages of rifting have been proposed for a given rifting event on a given rift segment, sometimes quite in disagreement with each other (Fig. 4). We therefore used the rating of the ages used to date extension, from weak to strong as described in section 4.2, to select the most reliable ages. To do so, we first considered for each rift segment the ages of a given extension period with highest rating. Then, several possibilities may occur. When the highest rating corresponds to a single date, it corresponds to the age reported in Fig. 8a. When several highest rating corresponding to time spans overlapping each other are available, we determined a mean age for the time span (e.g., mean age of 27.75 Ma for the Afar as the pre- and syn-rift age constraints are 29 and 26.5 Ma, respectively, as summarized in Supplementary Table S4). When rifting of a given period is dated by several time spans, several single dates or a combination of both with similar rating, we determined a mean age, taken as the likeliest ages of rift initiation (Supplementary Table S5; Fig. 8a).

We have calculated a series of weighted probability distributions (Kernel density estimations; Wessa, 2015) from the 25 ages of rift initiation, taking into account the robustness of the rifting age constraints into account (Supplementary Fig. S2; Fig. 8a; Supplementary Table S5). The probability distributions computed with smoothing bandwidth values ranging from 0.25 to 1.75 share five main peaks of rift initiation, whose mean ages are dated at 35.5, 27.6, 17, 10.7 and 5.7 Ma (Fig. 8b; Supplementary Table S6). The oldest peak corresponds to the extension that started during the Late Eocene in TBRZ and mainly led to the development of the Lokichar basin (Morley et al., 1999b). The second peak represents the onset of rifting recorded in the late Lower Oligocene in the northern part of the EARS (in Afar and TBRZ; Boschetto et al., 1992; Morley et al., 1992; Ukstins et al., 2002; Wolfenden et al., 2005; Macgregor, 2015), which was coeval with the uplift of the Ethiopian dome (Pik et al., 2003; Gani et al., 2009). The short, slight extension in the Rukwa rift during the Upper Oligocene developed slightly after this second period of rift initiation (Roberts et al., 2012b). The third peak dated at 17 Ma is found in several provinces of the East and West branches located around of the TBRZ (i.e., the TBRZ, the South MER, and the Nyanza, North Gregory and Albertine rifts; Fig. 8a; Drake et al., 1988; McDougall and Watkins, 1988; Boschetto et al., 1992; Ebinger et al., 1993a; Behrensmeyer et al., 2002; Simon et al., 2017). The tectonic activity was mostly characterized by slight faulting and basin downwarping and was synchronous with the uplift of the Kenya dome (Wichura et al., 2010). Importantly, these three older periods of extension were restricted to one or several segments of the EARS.

Contrary to the three older peaks, the two most recent peaks correspond to periods of generalized rifting that synchronously occurred all over EARS. The first period of generalized rift initiation started at 10.7 Ma and led to the development of grabens in the southern Afar, the North and Central MER, the North Gregory and Tanganyika rifts and the Mozambique channel (Crossley, 1979; Mougenot et al., 1989; Wolde-Gabriel et al., 1990; Cohen et al., 1993; Ukstins et al., 2002; Wolfenden et al., 2005). Around the Miocene - Pliocene transition (~5.7 Ma), the already active grabens of the EARS underwent a significant increase of

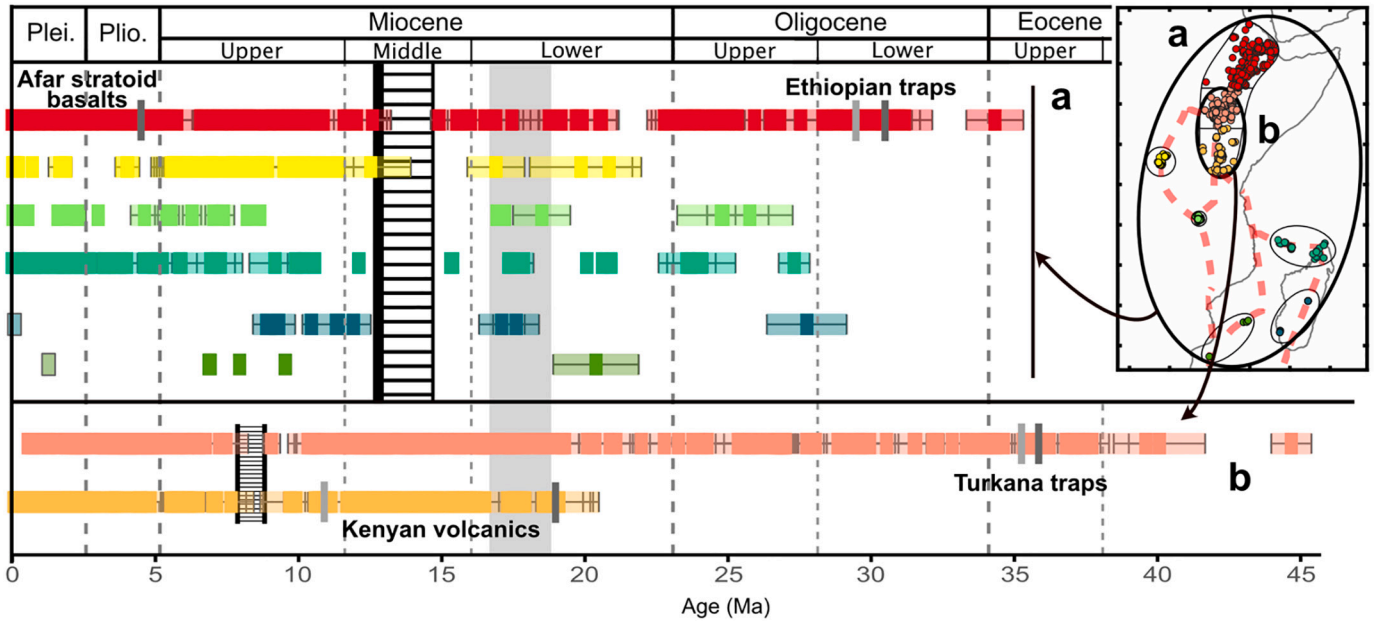

Fig. 7. Temporal distribution of the magmatic provinces of the West, South-East, Indian Ocean branches and the Afar-Ethiopian Plateau province (a), and the Turkana Broadly Rifted Zone (TBRZ) and Gregory – Nyanza Rift (GNR) provinces (b). Same colours as in Fig. 6. At the EARS' scale (a), the provinces share periods of coeval volcanic activity and hiatus between 12.5 and 15 Ma (hatched zone). The grey bar between 17 and 18.5 Ma accounts for a period of activity in almost all the provinces, i.e., except in the poorly dated South-East branch. The thick black line marks the coeval renewal of magmatism at 12–12.5 Ma in the three branches after the lull of activity. In the southern East branch (b), the TBRZ and GNR both recorded the main volcanic phase of the Kenyan volcanics, and short but representative hiatuses between 7.4 and 9.1 Ma (narrow hatched zone).

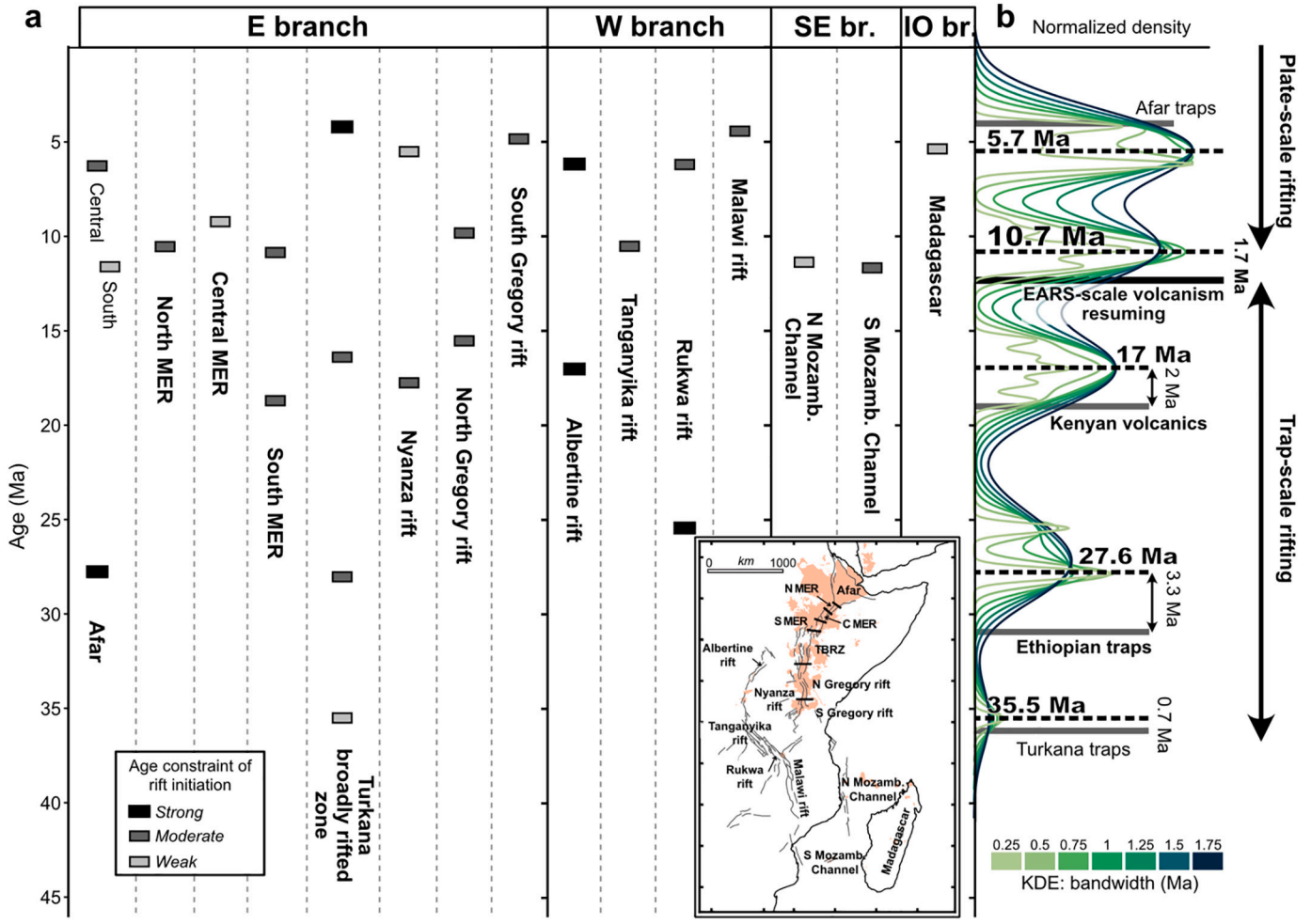

Fig. 8. a) Average age of rift initiation in the different segments of the EARS deduced from our critical review of ages published in the literature (Supplementary Table S5). b) Probability distributions (Kernel density estimation (KDE) with smoothing bandwidth ranging between 0.25 and 1.75 Ma; Wessa, 2015) of the periods of rift initiation at the scale of the EARS calculated from the 25 mean ages determined in Supplementary Table S5. The weighting procedure on the mean ages of rift initiation consists in applying a coefficient to the mean ages (1 to 3 for weak to strong age constraints; see Supplementary Table S5). The different probability curves are normalized to the main peak at 5.7 Ma. Note that KDEs performed with different smoothing bandwidth values (Supplementary Fig. S2) allow to determine a mean age for each main peak of rift initiation and reveal a maximum standard deviation of 0.35 for these peaks, which are consequently poorly sensitive to this parameter (Supplementary Table S6). The peaks on the probability density function, highlighted by dashed black lines, represent the mean age for the periods of rift initiation at the EARS' scale. Grey and black bars account for the trap and continental flood basalt events, and the resuming of the volcanism along the entire EARS, respectively.

subsidence (North Gregory and Albertine rifts and Mozambique channel; Spiegel et al., 2007; Franke et al., 2015; Simon et al., 2017), rift structures were reactivated (Afar, South MER, TBRZ, Nyanza and Rukwa rifts; Pickford, 1994; Ebinger et al., 1989b, 2000; Haileab et al., 2004; Stab et al., 2016), and new grabens initiated (South Gregory and Malawi rifts and Madagascar; Foster et al., 1997; Laville et al., 1998; McCartney and Scholz, 2016).

Our synthesis of rifting suggests the occurrence of two successive periods of rifting distinguished both from the extent of the areas synchronously affected by extension and from the magnitude and duration of extension (Fig. 8b).

6. Discussion

The cause of intraplate magmatism in continental areas is often subject to debate. Two endmember models propose that it may result either from deep-seated mantle plumes rooted in the core-mantle boundary (the "plume" theory; Morgan, 1971), or from lithospheric deformation related to plate tectonics without any input of lower mantle material (the "plate" theory; Anderson, 2000, 2005; Foulger, 2010). In the latter case, magmatism would stem from shallow thermal instabilities in the upper mantle (King and Ritsema, 2000) or from the collection of already existing partial melts in a heterogeneous upper mantle (Valentine and Perry, 2007; Valentine and Hirano, 2010; Brenna et al., 2012; Smith et al., 2021). In the context of lithospheric extension, asthenospheric decompression is an additional process for mantle partial melting and magma production (Ruppel, 1995).

In this general theoretical framework, the volcanism of the EARS has been interpreted in different ways, partly depending on the volume of emitted magmas. Deep mantle plumes would have caused the traps and flood basalts emitted during relatively short periods (1–7 Myrs) coeval with plateau uplift for the two most voluminous (Ethiopian traps and Kenyan volcanics; Ebinger and Sleep, 1998; George et al., 1998; Courtillot et al., 1999; Pik et al., 2006). The discontinuous small-volume volcanic activity in the West, South-East and Indian Ocean branches is more controversial. It is thought to be either the result of plume-fed lateral asthenospheric flows (Ebinger and Sleep, 1998), independent mantle plumes (Comoros archipelago; Emerick and Duncan, 1982; Class et al., 2005; Rungwe; Burke and Dewey, 1973), related to lithospheric extension (Corti et al., 2003), or remains unexplained as in Madagascar. Alternatively, geochemical data and tomographic images suggest that the volcanism of the whole EARS could arise from several mantle

anomalies rooted in the seismically imaged African Large Low Shear Velocity Province (LLSVP; Montelli et al., 2006; Furman, 2007; Halldórsson et al., 2014; Civiero et al., 2015; French and Romanowicz, 2015; O'Connor et al., 2019; Tsekhmistrenko et al., 2021). In this hypothesis of a common source for the volcanism, the genetic link with the lithospheric extension is unclear.

Our results suggest that the EARS experienced an overall similar timing of volcanism and rifting all over its provinces, overprinted by four short periods of intense magma emission on restricted areas (Turkana, Ethiopian plateau, Kenya and Afar; Figs. 6, 7). We saw above that such sporadic volcanism has been attributed to successive mantle plume head impingements below the African lithosphere (Hofmann et al., 1997; Ebinger and Sleep, 1998; George et al., 1998). However, as previously argued by Bailey (1992, 1993), the remarkable synchronicity of volcanism and tectonics in provinces spread over ~5000 km challenges the classical plume model, and raises fundamental questions about the relationship between lithospheric extension and mantle upwelling. Therefore, alternative interpretations suggest that the entire volcanism of the EARS results from the sole effect of successive events of plate deformation (e.g., Bailey and Woolley, 2005).

Here, we take advantage of our compilations of volcanism and extension ages to infer the respective roles of mantle and plate dynamics in the evolution of the EARS. Our synthesis suggests the occurrence of two successive periods distinguished by the extent of the areas synchronously affected by volcanism and extension, by the magnitude and duration of both phenomena (Figs. 8b and 9). We propose that the EARS is characterized by an Upper Eocene to Middle Miocene period of prevailing trap-scale rifting, during which extension was almost exclusively restricted to areas of continental flood basalts. This magmato-tectonic event is followed, since the Upper Miocene, by a period of plate-scale rifting that marks the onset of a widespread deformation in the four branches of the EARS.

When discussing the possible causes of both volcanism and extension and the origin of this twofold evolution, the seven following key features must be integrated to any hypothesis for rifting and magma production within the EARS.

1- As noted by Thorpe and Smith (1974), the volcanism and deformation almost systematically developed along Pan-African orogenic belts and avoided the cratonic regions (Fig. 2a). These belts have repeatedly focused thermal events and ascending magmas since the Proterozoic leading to the fertilization of the sub-continental lithospheric mantle (Wilson and Guiraud, 1992; Begg et al., 2009). Thus, the spatial distribution of both volcanism and tectonics suggests a main mechanical control of the lithosphere in the concentration of the deformation and in the channelization of the ascending magmas along the main inherited shear zones (e.g., Bailey, 1977; Corti et al., 2007).

2- Magmatism did not significantly migrate in each volcanic province (Bailey, 1992) while the African lithosphere drifted northwards of about 400–500 km since 25–27 Ma (George et al., 1998). The lack of any lateral displacement of the active volcanic centres seems in contradiction with the migration expected if each province was related to the sole effect of the mantle dynamics. It instead strengthens the role played by the lithospheric structures in the location of magma emission.

3- Synchronous magmatic activity occurs all-over the African plate. Wooley (2001) revealed that the magmatism of the African plate experienced periods of coeval activity since the Early Cretaceous. Our compilation concentrated on a shorter timescale, spanning from the Eocene to present, leads to a similar conclusion. The volcanism started in the East branch in the Eocene with two traps events (Turkana and Ethiopian flood basalts). Yet, it extended to the entire EARS as soon as the Upper Oligocene – Lower Miocene with a discontinuous, small-volume volcanic activity (Figs. 7, 9a). Furthermore, a pulse of volcanism from 18.5 to 17 Ma occurred in almost all the volcanic provinces, synchronously with the initiation of the emission of the Kenyan volcanics. Finally, the volcanism renewed at 12–12.5 Ma in most volcanic areas after a lull of activity between 15 and 12.5 Ma (Fig. 7). The volume of magma (relatively small but hardly quantifiable), the timing (a discontinuous volcanic activity since 25–27 Ma) and the lack of crustal doming are not compatible with the model of mantle plume of Morgan (1971). The onset of the volcanism between 25 and 27 Ma and its intensification at ~18.5 Ma in provinces of the EARS distant of about 5000 km can also be hardly explained by an Afar or Kenyan plume-fed,

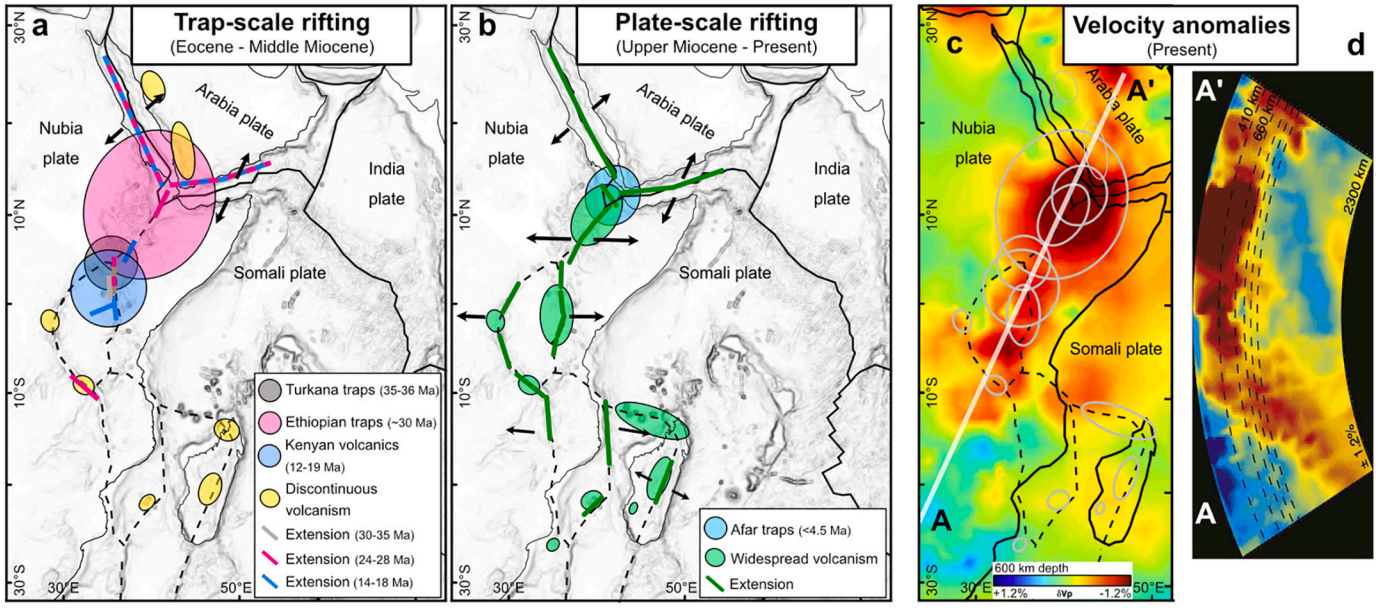

Fig. 9. Evolution of the EARS from a prevailing trap-scale rifting between the Eocene and Middle Miocene (a) to a plate-scale rifting since the Upper Miocene (b). The onset of a widespread volcanism around 12–12.5 Ma followed by a generalized rifting around 10.7 Ma mark the transition between the two extension dynamics. Extension directions from ArRajehi et al. (2010) for the Red Sea and Gulf of Aden and from Stamps et al. (2018) for the EARS. The EARS developed atop an abnormally hot upper mantle as shown by the P-wave velocity perturbations at 600 km depth (c; Hansen et al., 2012). The volcanic provinces of the EARS (light grey ellipses in c) are remarkably superimposed to a widespread upper mantle anomaly deepening southward in the LLSVP located in the lower mantle (d; Hansen et al., 2012). (For interpretation of the references to colour in this figure legend, the reader is referred to the web version of this article.)

fast-moving lateral asthenospheric flow like those producing age-progressive hotspot tracks in the southern Atlantics (O'Connor et al., 2018). Moreover, the apparent synchronicity of the widespread, discontinuous, and small-volume volcanism in the different branches of the EARS casts doubt on the existence of totally independent thermal anomalies at the origin of each volcanic province. Finally, the absence of known lithospheric extension in most segments that experienced this Upper Oligocene – Middle Miocene volcanism mostly disagrees with an asthenospheric decompression due to rift-related lithospheric thinning, as in passive rifts (Ruppel, 1995).

4- Our synthesis of the volcanic activity and the periods of rift initiation seems to indicate that the onset of volcanism predated the lithospheric deformation. During the period of predominant trap-scale rifting, the traps or major volcanic events were generally coeval with crustal doming and followed by extension spatially restricted to the vicinity of the volcanic zones (Fig. 9a). As rift initiation in the EARS was partly dated by volcanic units deposited within the grabens (providing a minimum age rated as weakly constrained), it cannot be totally excluded that its age was locally slightly underestimated. Yet, the weighting in the age probability estimates combined with the use of several smoothing bandwidths in the Kernel density estimations considerably minimizes the potential methodological biases and an uncertainty of ±1 Myr seems to be reasonably applied to the age of the periods of rift initiation. The volcanism/ extension succession begins with the Turkana traps, followed by extension in the Lokichar basin only by 0.7 Myrs, a too short interval to be considered significant given our dating strategy. Then, the Ethiopian traps volcanism was followed by ~3 Myrs by extension in Afar and TBRZ (Figs. 8b and 9a; Boschetto et al., 1992; Morley et al., 1992; Ukstins et al., 2002; Wolfenden et al., 2005; Macgregor, 2015), synchronously with the onset of the Ethiopian plateau's uplift (Pik et al., 2003; Gani et al., 2009). The same succession was observed in the Middle-Late Miocene with the Kenyan volcanics (flood basalts and ignimbrites; George et al., 1998; Tatsumi and Kimura, 1991) followed by 2 Myrs by the slight faulting and basin downwarping in several provinces of the East and West branches located in the vicinity of the uplifting Kenya Dome (i.e., the TBRZ, the South MER, and the Nyanza, North Gregory and Albertine rifts; Figs. 8 and 9a; Drake et al., 1988; McDougall and Watkins, 1988; Boschetto et al., 1992; Ebinger et al., 1993a; Behrensmeyer et al., 2002; Wichura et al., 2010; Simon et al., 2017). Our compilation also shows that a main change occurred in the dynamics of the EARS between 11 Ma and 12.5 Ma, with renewed volcanism at 12–12.5 Ma in all the volcanic provinces already affected by the volcanism, and followed, by 1.7 Myrs, by the onset of continuous and widespread rifting (Figs. 8b and 9b). Thus, volcanism seems to be systematically followed by extension in its surrounding areas. It may suggest that magmatism-related processes favour rifting in the EARS during both periods of prevailing trap-scale and plate-scale rifting.

5- Combining radiometric ages of the volcanism and the ages of rift initiation, we show that the EARS experienced successive magmato-tectonic events at 35.5, 27.5–30, 17–19, 11–12.5 and 5–6 Ma (Fig. 8b). Noteworthily, most of these events were coeval with the main changes in the geodynamics of the plate boundaries surrounding Africa. The age of 35 Ma corresponds to the onset of rifting in the Gulf of Aden (Bellahsen et al., 2006) and to a sharp increase of the spreading rate in the South-West Indian ridge (SWIR; Fig. 10; DeMets et al., 2021). The opening of the Red Sea started at 27 Ma synchronously with extension around the area covered by the Ethiopian traps (Bosworth et al., 2005) and slightly before the extension in the Rukwa rift (Roberts et al., 2012b). The onset of seafloor spreading in the Gulf of Aden is dated at 17.5 Ma (Fournier et al., 2010) and the changes of spreading rates along the ridges surrounding the Nubia and Somali plates (DeMets and Merkouriev, 2019; DeMets et al., 2020, 2021) were all coeval with the initiation of magmatic periods and/or extension in the EARS (Fig. 10). The widespread volcanic resumption and rifting at 11–12.5 in the EARS is contemporaneous with changes of the spreading rates in the southern Atlantic (DeMets and Merkouriev, 2019) and the Indian Ocean (Merkouriev and DeMets, 2006; Fournier et al., 2010; DeMets et al., 2020), the migration of the rotation pole of the India-Somalia and Capricorn-

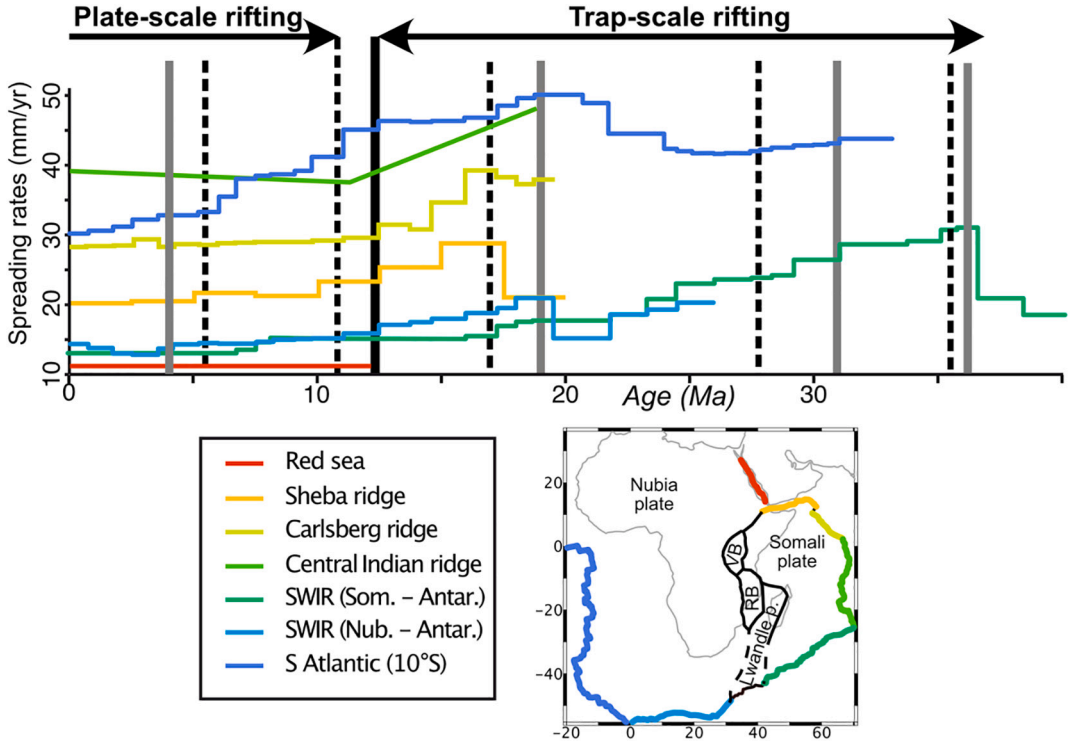

Fig. 10. Spreading rates along the ridges bounding the Nubia and Somali plates (Merkouriev and DeMets, 2006; Fournier et al., 2010; DeMets and Merkouriev, 2019; DeMets et al., 2020, 2021; Augustin et al., 2021). Note the changes in the spreading rate gradients coeval with the main magmato-tectonic events represented as in Fig. 8. RB: Rovuma block; VB: Victoria block.

Somalia plate pairs (Merkouriev and DeMets, 2006; DeMets et al., 2020), and the beginning of the oceanic spreading in Red Sea (Augustin et al., 2021).

6- Seismological images computed from regional and/or global seismic networks have all revealed low-velocity anomalies of various size and intensity in the upper and lower mantles beneath eastern Africa (Anderson et al., 1992; King and Ritsema, 2000; Montelli et al., 2006; Montagner et al., 2007; Begg et al., 2009; Civiero et al., 2015; Tsekhmistrenko et al., 2021). These anomalies, which are superimposed to the volcanic provinces of the EARS (Fig. 9c), are in geometric connection with the LLSVP beneath southern Africa (Ritsema et al., 1999; Hansen et al., 2012; Tsekhmistrenko et al., 2021; Fig. 9d).

If the occurrence of low-velocity anomalies is widely accepted, their nature is highly debated (e.g., Garnero et al., 2016). On the one hand, the LLSVP below southern Africa is interpreted as a large thermal anomaly broken up into bundles of thermomechanical plumes (Davaille and Romanowicz, 2020), which promotes an ascending flow from the lower mantle (Forte et al., 2010), feeds mantle anomalies within the upper mantle (e.g., Civiero et al., 2015), and/or triggers the development of plume-like discrete mantle anomalies on their margins (e.g., Torsvik et al., 2006; Burke et al., 2008; Tsekhmistrenko et al., 2021). On the other hand, the LLSVP is considered as a large compositional anomaly with mantle volumes richer in iron, hence denser than the rest of the mantle and not thermally buoyant (e.g., Trampert et al., 2004). An alternative interpretation suggests that the LLSVP is primarily a thermal anomaly with a basal positive density anomaly (Simmons et al., 2010). Whatever the amplitude of the dense compositional anomaly, Ishii and Tromp (1999) and Mao et al. (2006) proposed that the LLSVP could correspond to zones of concentration of dense iron-rich materials, but the iron enrichment would stem from an iron concentration beneath mantle upwellings. Thus, the possible iron-rich origin of a dense LLSVP would be compatible with ascending materials above this anomaly.

The low-velocity anomalies imaged in the upper mantle below the volcanic provinces of the EARS are widely considered as evidence of hot mantle volumes (e.g., Anderson et al., 1992; Montagner et al., 2007; Civiero et al., 2015). Yet, the temperature estimates of these mantle anomalies suggest thermal anomalies toward the lower end of the global temperature range for large igneous provinces, despite markedly slow seismic velocities of the mantle that underlies the regions (Rooney et al., 2012). It could therefore suggest that the low seismic velocities underneath Africa reflect the occurrence upper mantle thermal anomalies containing carbonatite (i.e., CO_2-assisted) melting (Presnall and Gudfinnsson, 2005; Dasgupta and Hirschmann, 2006; Rooney et al., 2012).

7- Finally, the geochemical signatures of the lavas emitted along the EARS reveal the involvement of different mantle sources in the magma production (e.g., Class et al., 1998; Rogers et al., 2000; Pik et al., 2006; Furman, 2007). These sources are proposed to originate from the African LLSVP, which is thought to compositionally heterogeneous (Furman, 2007; Meshesha and Shinjo, 2008; Halldórsson et al., 2014). Interestingly, this interpretation based on samples restricted to the East and West branches, was confirmed by O'Connor et al. (2019) when integrating volcanic products of the four branches. Indeed, the authors identified a unique non-volatile superplume isotopic signature in the post-10 Ma magmas emitted during the plate-scale rifting.

The above-mentioned synthesis of the seven key features suggests that the structure and evolution of the EARS, and the dynamics of the surrounding plates and underneath mantle cannot be explained with the sole "plume" or sole "plate" theories. We therefore interpret the EARS as the result of the combined effects of (1) extensive stresses acting on the African lithosphere in the long-lived context of the Gondwana breakup and (2) an overall complex dynamics of mantle upwelling.

The extensive stresses could arise from far-field stresses, variations of GPE, and/or divergent shear traction exerted at the base of the Nubia and Somali lithospheres (e.g., Forte et al., 2010; Ghosh and Holt, 2012; Stamps et al., 2015). According to Stamps et al. (2015), the current kinematics of the EARS results from the combined effects of GPE variations and Couette-type divergent mantle flow. Yet, it is worth noting that extension stresses due to GPE variations cannot be invoked for rifting periods prior to any uplift event like for the Turkana extension at around 35 Ma.

It is also important to mention that the mantle upwellings beneath Africa clearly differ from the narrow plumes of Morgan's theory (1971). The mantle dynamics could instead correspond to a global upward and north-easterly tilted mantle flow (Forte et al., 2010; Hansen et al., 2012; Fig. 9d) made of bundles of compositional and/or thermal anomalies of different size and magnitude originating from the African LLSVP (Davaille and Romanowicz, 2020).

In such a general context, we propose that the LLSVP may have spewed thermal and/or compositional anomalies of various sizes, intensities, and compositions in an upper mantle becoming hotter than normal. We speculate that their surface expression (i.e., volcanism) was partly modulated by extension stresses arising from the plate circuit and/or basal lithospheric drag due to divergent mantle flows as suggested by the synchronicity between, on the one hand, the tectono-magmatic events of the EARS at 35.5, 17–19, 11–12.5 Ma, and, on the other hand, changes in the dynamics along the Nubia and Somali plates boundaries (Fig. 10).

The following gradation of mantle anomalies vs. extension stresses can be proposed to explain the evolution of the EARS. The first endmember corresponds to a main role played by the mantle anomalies in the development of the volcanic event. This case is well illustrated by the Ethiopian traps that were followed by extension in the adjacent segments, including the Gulf of Aden and the Red Sea (Courtillot et al., 1999; Bosworth et al., 2005). The lack of any evolution of the spreading rates in the oceanic ridges at that time around the Somali and Nubia plates (Fig. 10) suggests that the development of the Ethiopian traps followed by rifting does not result from the increase of plate-scale extension stresses, but instead from a dynamic mantle anomaly.

The second endmember is characterized by a dominant role of the plate deformation in the location and timing of the volcanism. Following Presnall and Gudfinnsson (2005) and Rooney et al. (2012) who suggested that the slow seismic velocities could evidence the occurrence of carbonatite melts in the upper mantle, we propose that the ascent of carbonatite melts from the lower mantle to the upper mantle beneath Africa has produced widespread carbonated silicate melts at shallow depth having compositions similar to the alkaline magmas emitted in the volcanic provinces of the EARS (Kampunzu and Mohr, 1991; Rudnick et al., 1993; Coltorti et al., 1999; Dasgupta et al., 2007; Furman, 2007; Mazzeo et al., 2021). Moreover, the widespread distribution of easily fusible lithospheric metasomes within the continental lithosphere mantle might have facilitated magma generation without the need for substantial lithospheric thinning or elevated mantle potential temperatures (Rooney et al., 2014). Thus, a deformation-driven collection of already existing partial melts in a heterogenous mantle, as described by Valentine and Perry (2007), Spera and Fowler (2009) Valentine and Hirano (2010), Smith et al. (2021), could have produced a tectonically controlled magmatism. We therefore interpret the timing of the alkaline volcanism along the Pan-African mobile belts, synchronously with main changes in the spreading ridge dynamics, as primarily controlled by the increase of extension stresses. To this respect, the Late Oligocene extension in the Rukwa rift (Fig. 8), coeval with a small alkaline to carbonatitic volcanic activity (E.M. Roberts et al., 2012b), would stem from a period of increasing extension stresses in the African lithosphere.

The occurrence of (1) the Turkana traps at around 35 Ma (without any lithospheric doming) and (2) the Kenyan volcanics and a widespread volcanic renewal initiated around 19 Ma (Fig. 7), while the spreading ridges recorded modifications in the extension rates (Fig. 10), might be explained by the massive melting of fertile mantle heterogeneities triggered by lithospheric deformation.

Our synthesis can hardly determine whether the extension stresses primarily stem from far field stresses or divergent mantle flow. However, considering the main Middle Miocene change in the EARS evolution, i.

e., from a prevailing trap-scale to a plate-scale rifting, we speculate that an increase of large-scale ascending mantle flow in the general framework of mantle convection during the Middle Miocene may have (1) augmented the mantle melting below all the volcanic provinces, (2) induced the Middle Miocene - Pliocene uplift of the Central African Plateau and Madagascar (de Wit, 2003; Ritsema et al., 2010; G.G. Roberts et al., 2012a; Daly et al., 2020), (3) triggered the subsequent resumption of volcanism at 12–12.5 Ma, (4) enhanced pre-existing extensional stresses within the lithosphere by a stronger basal lithospheric drag due to a divergent Couette-type mantle flow within the sub-African asthenosphere combined to GPE variations (Stamps et al., 2015), and eventually (5) produced enough magmatism to reduce the strength of the continental lithosphere and promote magma-assisted rifting since ~11 Ma. This geodynamic change could have been important enough to modify the dynamics of the surrounding spreading ridges. Furthermore, the plate-motion change of the Capricorn plate, attributed to an increasing buoyancy of the Réunion plume flux at 11 Ma (Iaffaldano et al., 2018), could instead result from the main change of the dynamics of the EARS in tandem with the possible increase of the sub-lithospheric mantle flux. The magmatic pulse recently evidenced along the Sheba ridge at 11 Ma (Gillard et al., 2021) could also have an origin closely linked to the evolution of the EARS. We finally suggest that the source of extension stresses affecting the African plate progressively evolved from a dominant far-field origin to prevailing GPE variations and a diverging Couette-type basal shear, thus changing of the dynamics of the EARS from trap-scale to plate scale rifting. In such a context of ascending mantle flux and increasing extension, the areas with a significant lithospheric thinning likely met extremely favourable conditions to produce large magma volumes like in Afar since 5 Ma (Bastow and Keir, 2011; Armitage et al., 2015).

7. Conclusion

Our study on the magmato-tectonic relationship of the EARS allowed us to update its geometry, by including the Mozambique channel and Madagascar in the rift system. The EARS is thus composed of one magma-rich segment, the East branch, and three magma-poor segments, the West, South-East, and Indian Ocean branches, which all delimit independent lithospheric blocks. We have built a comprehensive database of volcanic ages made from a thorough selection of the published isotopic ages of volcanism emitted along the four branches since the Middle Eocene. This compilation reveals an overall similar timing of relative quiescence (12.5–15 Ma) and renewals (17–18.5 and 12–12.5 Ma) of activity in the different volcanic provinces, overprinted by four short (1–7 Ma) periods of intense magma emission on 500–1000 km-wide areas (Turkana, Ethiopian plateau, Kenya and Afar). We also compiled the periods of rift initiation published in the literature and evaluated the geological constrains to date them. This critical review provides insights on the timing of extension at the EARS' scale and suggests the occurrence of five successive periods of extension since the Upper Eocene. Combining the spatio-temporal distribution of both volcanism and rifting, we show that the African plate dismantling results from the intricate relationship between mantle and plate processes during two successive periods called trap-scale and plate-scale rifting between the Upper Eocene - Middle Miocene and Upper Miocene – Holocene, respectively (Figs. 8 and 9).

We summarize seven key features suggesting that the EARS' evolution cannot be explained by the sole plume or sole plate theories as defined by Anderson (2005). From these seven features, we propose an intermediate interpretation in which the EARS results from the intricate relationship between the mantle and plate dynamics. We consider the African LLSVP as a thermo-compositional deep anomaly that feeds mantle anomalies of different composition, size and magnitude in an overall ascending and north-easterly tilted mantle flow. This mantle dynamics likely brought favourable conditions to promote the widespread production of carbonated silicate melts emitted as alkaline magmas along the four branches of the EARS and massive volumes of tholeiitic melts feeding the trap events. The synchronicity between most of the magmato-tectonic events in the EARS and changes in the dynamics of the Nubia and Somali plates boundaries suggests that extension stresses affecting the African lithosphere partly modulated the melting of the mantle anomaly and/or the collection of magma through the Pan-African belts. The sole exception corresponds to the Ethiopian trap event and the subsequent rifting in the surrounding areas that was not coeval with modifications in the dynamics of the plate boundaries.

Finally, the source of extension stresses affecting the African plate probably evolved from a dominant far-field origin to prevailing GPE variations and a diverging Couette-type basal shear. We propose that this change results from the increase of the mantle flux in the Middle Miocene, yielding an evolution of the dynamics of the EARS from trap-scale to plate scale rifting.

Supplementary data to this article can be found online at https://doi.org/10.1016/j.earscirev.2022.104089.

Declaration of Competing Interest

The authors declare that they have no known competing financial interests or personal relationships that could have appeared to influence the work reported in this paper.

Acknowledgments

The authors want to warmly thank G. Foulger, D. Franke, A. Moore and an anonymous reviewer for their very constructive reviews that contributed to considerably improve the initial version of this manuscript. This work was supported by the Université de La Réunion.

References

Anderson, D.L., 2000. The thermal state of the upper mantle; no role for mantle plumes. Geophys. Res. Lett. 27, 3623–3626.

Anderson, D.L., 2005. Scoring hotspots: The plume and plate paradigms. In: Foulger, G. R., Natland, J.H., Presnall, D.C., Anderson, D.L. (Eds.), Plates, Plumes and Paradigms. Geological Society of America, Spec. papers, 388, pp. 31–54. https://doi.org/10.1130/0-8137-2388-4.31.

Anderson, D.L., Zhang, Y.-S., Tanimoto, T., 1992. Plume heads, continental lithosphere, flood basalts and tomography. In: Storey, B.C., Alabster, T., Pankhurst, R.J. (Eds.), Magmatism and the Causes of Continental Break-Up, Geol. Soc. Spe. Pub., London, 68, pp. 99–124.

Armitage, J.J., Ferguson, D.J., Goes, S., Hammond, J.O.S., Calais, E., Rychert, C.A., Harmon, N., 2015. Upper mantle temperature and the onset of extension and break-up in Afar, Africa. Earth Planet. Sci. Lett. 418, 78–90. https://doi.org/10.1016/j.epsl.2015.02.039.

ArRajehi, A., McClusky, S., Reilinger, R., Daoud, M., Alchalbi, A., Ergintav, S., Gomez, F., Sholan, J., Bou-Rabee, F., Ogubazghi, G., Haileab, B., Fisseha, S., Asfaw, L., Mahmoud, S., Rayan, A., Bendik, R., Kogan, L., 2010. Geodetic constraints on present-day motion of the Arabian Plate: Implications for Red Sea and Gulf of Aden rifting. Tectonics 29, TC3011.

Augustin, N., van der Zwan, F.M., Devey, C.W., Brandsdóttir, B., 2021. 13 million years of seafloor spreading throughout the Red Sea Basin. Nat. Commun. 12, 2427.

Bailey, D.K., 1977. Lithosphere control of continental rift magmatism. J. Geol. Soc. 133, 103–106. https://doi.org/10.1144/gsjgs.133.1.0103.

Bailey, D.K., 1992. Episodic alkaline igneous activity across Africa: implications for the causes of continental break-up. Geol. Soc. Lond., Spec. Publ. 68, 91–98.

Bailey, D.K., 1993. Carbonate magmas. J. Geol. Soc. 150, 637–651.

Bailey, D.K., Woolley, A.R., 2005. Repeated, synchronous magmatism within Africa: Timing, magnetic reversals, and global tectonics. In: Foulger, G.R., Natland, J.H., Presnall, D.C., Anderson, D.L. (Eds.), Plates, Plumes, and Paradigms. Geological Society of America, Special Papers, pp. 365–377. https://doi.org/10.1130/2005.2388(22).

Balestrieri, M.L., Bonini, M., Corti, G., Sani, F., Philippon, M., 2016. A refinement of the chronology of rift-related faulting in the Broadly Rifted Zone, southern Ethiopia, through apatite fission-track analysis. Tectonophysics 671, 42–55. https://doi.org/10.1016/j.tecto.2016.01.012.

Bastow, I.D., Keir, D., 2011. The protracted development of the continent-ocean transition in Afar. Nat. Geosci. 4, 248–250.

Begg, G.C., Griffin, W.L., Natapov, L.M., O'Reilly, S.Y., Grand, S.P., O'Neill, C.J., Hronsky, J.M.A., Djomani, Y.P., Swain, C.J., Deen, T., Bowden, P., 2009. The lithospheric architecture of Africa: Seismic tomography, mantle petrology, and tectonic evolution. Geosphere 5, 23–50. https://doi.org/10.1130/GES00179.1.

Behrensmeyer, A.K., Deino, A.L., Hill, A., Kingston, J.D., Saunders, J.J., 2002. Geology and geochronology of the middle Miocene Kipsaramon site complex, Muruyur Beds, Tugen Hills, Kenya. J. Hum. Evol. 42, 11–38.
Bellahsen, N., Fournier, M., d'Acremont, E., Leroy, S., Daniel, J.M., 2006. Fault reactivation and rift localization: Northeastern Gulf of Aden margin. Tectonics 25, TC1007. https://doi.org/10.1029/2004TC001626.
Berthod, C., Bachèlery, P., Jorry, S.J., Pitel-Roudaut, M., Ruffet, G., Revillon, S., Courgeon, S., Doucelance, R., 2022. First characterization of the volcanism in the southern Mozambique Channel: Geomorphological and structural analyses. Mar. Geol. 445, 106755.
Bertil, D., Regnoult, J.-M., 1998. Seismotectonics of Madagascar. Tectonophysics 294, 57–74.
Bertil, D., Mercury, N., Doubre, C., Lemoine, A., Van der Woerd, J., 2021. The unexpected Mayotte 2018–2020 seismic sequence: a reappraisal of the regional seismicity of the Comoros. Compt. Rendus Geosci. 353 https://doi.org/10.5802/crgeos.79.
Bésairie, H., 1960. Lexique Stratigraphique International (vol. IV, Afrique, Fsc. 11, Madagascar, 190 p).
Bialas, R.W., Buck, W.R., Qin, R., 2010. How much magma is required to rift a continent? Earth Planet. Sci. Lett. 292, 68–78. https://doi.org/10.1016/j.epsl.2010.01.021.
Bonini, M., Corti, G., Innocenti, F., Manetti, P., Mazzarini, F., Abebe, T., Pecskay, Z., 2005. Evolution of the Main Ethiopian Rift in the frame of Afar and Kenya rifts propagation. Tectonics 24. https://doi.org/10.1029/2004TC001680 n/a-n/a.
Boone, S.C., Seiler, C., Kohn, B.P., Gleadow, A.J.W., Foster, D.A., Chung, L., 2018. Influence of rift superposition on lithospheric response to East African Rift System Extension: Lapur Range, Turkana, Kenya. Tectonics 119, 120–126. https://doi.org/10.1002/2017TC004575.
Boschetto, H.B., Brown, F.H., McDougall, I., 1992. Startigraphy of the Lothidok Range, northern Kenya, and K/Ar ages of its Miocene primates. J. Hum. Evol. 22, 47–71.
Bosworth, W., 1992. Mesozoic and early Tertiary rift tectonics in East Africa. Tectonophysics 209, 115–137.
Bosworth, W., Huchon, P., McClay, K., 2005. The Red Sea and Gulf of Aden Basins. J. Afr. Earth Sci. 43, 334–378. https://doi.org/10.1016/j.jafrearsci.2005.07.020.
Brenna, M., Cronin, S.J., Smith, I.E.M., Maas, R., Sohn, Y.K., 2012. How Small-volume Basaltic Magmatic Systems Develop: a Case Study from the Jeju Island Volcanic Field, Korea. J. Pet. 53, 985–1018. https://doi.org/10.1093/petrology/egs007.
Bromage, T.G., Schrenk, F., Juwayeyi, Y.M., 1995. Paleobiogeography of the Malawi Rift: age and vertebrate paleontology of the Chiwondo Beds, northern Malawi. J. Hum. Evol. 28, 37–57.
Burke, K., Dewey, J.F., 1973. Plume-generated triple junctions: key indicators in applying plate tectonics to old rocks. J. Geol. 81, 406–433. http://www.jstor.org/stable/30070631.
Burke, K., Steinberger, B., Torsvik, T.H., Smethurst, M.A., 2008. Plume generation zones at the margins of Large Low Shear Velocity Provinces on the core–mantle boundary. Earth Planet. Sci. Lett. 265, 49–60. https://doi.org/10.1016/j.epsl.2007.09.042.
Calais, E., Ebinger, C., Hartnady, C., Nocquet, J.M., 2006. Kinematics of the East African Rift from GPS and Earthquake Slip Vector Data. Geol. Soc., Lond., Spec. Publ. 259, pp. 9–22.
Castaing, C., 1991. Post-Pan-African tectonic evolution of South Malawi in relation to the Karroo and Recent East African Rift Systems. Tectonophysics 191, 55–73.
Catuneanu, O., Wopfner, H., Eriksson, P.G., Cairncross, B., Rubidge, B.S., Smith, R.M.H., Hancox, P.J., 2005. The Karoo basins of south-central Africa. J. Afr. Earth Sci. 43, 211–253. https://doi.org/10.1016/j.jafrearsci.2005.07.007.
Chorowicz, J., 2005. The East African rift system. J. Afr. Earth Sci. 43, 379–410. https://doi.org/10.1016/j.jafrearsci.2005.07.019.
Civiero, C., Hammond, J.O.S., Goes, S., Fishwick, S., Ahmed, A., Ayele, A., et al., 2015. Multiple mantle upwellings in the transition zone beneath the northern East-African Rift system from relative P-wave travel-time tomography. Geochem. Geophys. Geosyst. 16, 2949–2968. https://doi.org/10.1002/2015GC005948.
Class, C., Goldstein, S.L., Altherr, R., Bachèlery, P., 1998. The process of plume–lithosphere interactions in the ocean basins—the case of Grande Comore. J. Pet. 39, 881–903.
Class, C., Goldstein, S.L., Stute, M., Kurz, M.D., Schlosser, P., 2005. Grand Comore Island: a well-constrained "low 3He/4He" mantle plume. Earth Planet. Sci. Lett. 233, 391–409. https://doi.org/10.1016/j.epsl.2005.02.029.
Cochran, J.R., 1988. Somali Basin, Chain Ridge, and origin of the Northern Somali Basin gravity and geoid low. J. Geophys. Res. Solid Earth 93, 11985–12008.
Coffin, M.F., Rabinowitz, P.D., 1987. Reconstruction of Madagascar and Africa: evidence from the Davie fracture zone and western Somali basin. J. Geophys. Res. Solid Earth 92, 9385–9406.
Cohen, A.S., Soreghan, M.J., Scholz, C.A., 1993. Estimating the age of formation of lakes: an example from Lake Tanganyika, East African Rift system. Geology 21, 511–514.
Coltorti, M., Bonadiman, C., Siena, F., Upton, B.G.J., 1999. Carbonatite metasomatism of the oceanic upper mantle: evidence from clinopyroxenes and glasses in ultramafic xenoliths of Grande Comore, Indian Ocean. J. Petrol. 40, 133–165.
Corti, G., Bonini, M., Conticelli, S., Innocenti, F., Manetti, P., Sokoutis, D., 2003. Analogue modelling of continental extension: a review focused on the relations between the patterns of deformation and the presence of magma. Earth-Sci. Rev. 63, 169–247.
Courgeon, S., Jorry, S.J., Camoin, G.F., BouDagher-Fadel, M.K., Jouet, G., Révillon, S., Bachèlery, P., Pelleter, E., Borgomano, J., Poli, E., Droxler, A.W., 2016. Growth and demise of Cenozoic isolated carbonate platforms: New insights from the Mozambique channel seamounts (SW Indian Ocean). Mar. Geol. 380, 90–105. https://doi.org/10.1016/j.margeo.2016.07.006.
Courgeon, S., Jorry, S.J., Jouet, G., Camoin, G., BouDagher-Fadel, M.K., Bachèlery, P., Caline, B., Boichard, R., Révillon, S., Thomas, Y., Thereau, E., Guérin, C., 2017. Impact of tectonic and volcanism on the Neogene evolution of isolated carbonate platforms (SW Indian Ocean). Sediment. Geol. 355, 114–131.
Corti, G., van Wijk, J., Cloetingh, S., Morley, C.K., 2007. Tectonic inheritance and continental rift architecture: Numerical and analogue models of the East African Rift system. Tectonics 26 (6), TC6006. https://doi.org/10.1029/2006TC002086.
Courgeon, S., Bachèlery, P., Jouet, G., Jorry, S.J., Bou, E., BouDagher-Fadel, M.K., Révillon, S., Camoin, G., Poli, E., 2018. The offshore east African rift system: new insights from the Sakalaves seamounts (Davie Ridge, SW Indian Ocean). Terra Nova 15, 380–388. https://doi.org/10.1111/ter.12353.
Courtillot, V., Jaupart, C., Manighetti, I., Tapponnier, P., Besse, J., 1999. On causal links between flood basalts and continental breakup. Earth Planet. Sci. Lett. 166, 177–195.
Crossley, R., 1979. The Cenozoic stratigraphy and structure of the western part of the rift valley in southern Kenya. J. Geol. Soc. 136, 393–405.
Daly, M.C., Green, P., Watts, A.B., Davies, O., Chibesakunda, F., Walker, R., 2020. Tectonics and landscape of the Central African Plateau and their implications for a Propagating Southwestern Rift in Africa. Geochem. Geophys. Geosyst. 21 https://doi.org/10.1029/2019GC008746 e2019GC008746.
Dasgupta, R., Hirschmann, M.M., 2006. Melting in the Earth's deep upper mantle caused by carbon dioxide. Nature 440, 659–662. https://doi.org/10.1038/nature04612.
Dasgupta, R., Hirschmann, M.M., Smith, N.D., 2007. Partial melting experiments of peridotite + CO_2 at 3 GPa and genesis of alkalic ocean basalts. J. Petrol. 48, 2093–2124.
Davaille, A., Romanowicz, B., 2020. Deflating the LLSVPs: Bundles of mantle thermochemical plumes rather than thick stagnant "piles". Tectonics 39. https://doi.org/10.1029/2020TC006265 e2020TC006265.
de Wit, M.J., 2003. MADAGASCAR: heads it's a continent, tails it's an island. Annu. Rev. Earth Planet. Sci. 31, 213–248. https://doi.org/10.1146/annurev.earth.31.100901.141337.
DeMets, C., Merkouriev, S., 2019. High-resolution reconstructions of South America plate motion relative to Africa, Antarctica and North America: 34 Ma to present. Geophys. J. Int. 217, 1821–1853.
DeMets, C., Merkouriev, S., Jade, S., 2020. High-resolution reconstructions and GPS estimates of India–Eurasia and India–Somalia plate motions: 20 Ma to the present. Geophys. J. Int. 220, 1149–1171. https://doi.org/10.1093/gji/ggz508.
DeMets, C., Merkouriev, S., Sauter, D., 2021. High resolution reconstructions of the Southwest Indian Ridge, 52 Ma to present: implications for the breakup and absolute motion of the Africa plate. Geophys. J. Int. 226, 1461–1497.
Deville, E., Marsset, T., Courgeon, S., Jatiault, R., Ponte, J.-P., Thereau, E., Jouet, G., Jorry, S.J., Droz, L., 2018. Active fault system across the oceanic lithosphere of the Mozambique Channel: implications for the Nubia–Somalia southern plate boundary. Earth Planet. Sci. Lett. 502, 210–220. https://doi.org/10.1016/j.epsl.2018.08.052.
Drake, R.E., Van Couvering, J.A., Pickford, M.H., Curtis, G.H., Harris, J.A., 1988. New chronology for the Early Miocene mammalian faunas of Kisingiri, Western Kenya. J. Geol. Soc. 145, 479–491.
Ebinger, C.J., Sleep, N.H., 1998. Cenozoic magmatism throughout east Africa resulting from impact of a single plume. Nature 395, 788–791.
Ebinger, C.J., Bechtel, T.D., Forsyth, D.W., Bowin, C.O., 1989a. Effective elastic plate thickness beneath the East African and Afar plateaus and dynamic compensation of the uplifts. J. Geophys. Res. 94, 2883–2901.
Ebinger, C.J., Deino, A.L., Drake, R.E., Tesha, A.L., 1989b. Chronology of volcanism and rift basin propagation: Rungwe volcanic province, East Africa. J. Geophys. Res. 94, 15785–15803.
Ebinger, C.J., Yemane, T., WoldeGabriel, G., Aronson, J.L., Walter, R.C., 1993a. Late Eocene–Recent volcanism and faulting in the southern main Ethiopian rift. J. Geol. Soc. 150, 99–108.
Ebinger, C.J., Deino, A.L., Tesha, A.L., Becker, T., Ring, U., 1993b. Tectonic controls on rift basin morphology: evolution of the Northern Malawi (Nyasa) Rift. J. Geophys. Res. 98, 17821–17836.
Ebinger, C.J., Yemane, T., Harding, D.J., Tesfaye, S., Kelley, S., Rex, D.C., 2000. Rift deflection, migration, and propagation: linkage of the Ethiopian and Eastern rifts, Africa. Geol. Soc. Am. Bull. 112, 163–176.
Emerick, C.M., Duncan, R.A., 1982. Age progressive volcanism in the Comores Archipelago, western Indian Ocean and implications for Somali plate tectonics. Earth Planet. Sci. Lett. 60, 415–428.
Evernden, J.F., Curtis, G.H., Kistler, R.W., 1957. Potassium-argon dating of Pleistocene volcanics. Quaternaria 5, 348–385.
Fairhead, J.D., Mitchell, J.G., Williams, L.A.J., 1972. New K/Ar determinations of rift volcanics of S Kenya and the bearing of age of rift faulting. Nature 238, 66–69.
Famin, V., Michon, L., Bourhane, A., 2020. The Comoros archipelago: a right-lateral transform boundary between the Somalia and Lwandle plates. Tectonophysics 789, 228539. https://doi.org/10.1016/j.tecto.2020.228539.
Fitch, F.J., Hooker, P.J., Miller, J.A., Mitchell, J.G., Watkins, R.T., 1985. Reconnaissance potassium-argon geochronology of the Suregei-Asille district, northern Kenya. Geol. Mag. 122, 609–622.
Forte, A.M., Quéré, S., Moucha, R., Simmons, N.A., Grand, S.P., Mitrovica, J.X., Rowley, D.B., 2010. Joint seismic–geodynamic-mineral physical modelling of African geodynamics: a reconciliation of deep-mantle convection with surface geophysical constraints. Earth Planet. Sci. Lett. 295, 329–341. https://doi.org/10.1016/j.epsl.2010.03.017.
Foster, A., Ebinger, C., Mbede, E., Rex, D., 1997. Tectonic development of the northern Tanzanian sector of the East African Rift System. J. Geol. Soc. 154, 689–700.
Foulger, G.R., 2010. Plates vs Plumes: A Geological controversy. Wiley-Blackwell (364p).
Fournier, M., Chamot-Rooke, N., Petit, C., Huchon, P., Al-Kathiri, A., Audin, L., et al., 2010. Arabia-Somalia plate kinematics, evolution of the Aden-Owen-Carlsberg triple

junction, and opening of the Gulf of Aden. J. Geophys. Res. 115, B04102. https://doi.org/10.1029/2008JB006257.
Franke, D., Jokat, W., Ladage, S., Stollhofen, H., Klimke, J., Lutz, R., et al., 2015. The offshore East African Rift System: Structural framework at the toe of a juvenile rift. Tectonics 34. https://doi.org/10.1002/2015TC003922, 2086–2014.
French, S.W., Romanowicz, B., 2015. Broad plumes rooted at the base of the Earth's mantle beneath major hotspots. Nature 525, 95–99. https://doi.org/10.1038/nature14876.
Furman, T., 2007. Geochemistry of East African Rift basalts: an overview. J. Afr. Earth Sci. 48, 147–160. https://doi.org/10.1016/j.jafrearsci.2006.06.009.
Gani, N.D., Abdelsalam, M.G., Gera, S., Gani, M.R., 2009. Stratigraphic and structural evolution of the Blue Nile Basin, Northwestern Ethiopian Plateau. Geol. J. 44, 30–56. https://doi.org/10.1002/gj.1127.
Garnero, E.J., McNamara, A.K., Shim, S.-H., 2016. Continent-size anomalous zones with low seismic velocity at the base of Earth's mantle. Nat. Geosci. 9, 481–489.
George, R., Rogers, N., Kelley, S., 1998. Earliest magmatism in Ethiopia: evidence for two mantle plumes in one flood basalt province. Geology 26, 923–926.
Ghosh, A., Holt, W.E., 2012. Plate motions and stresses from global dynamic models. Science 335, 838–843. https://doi.org/10.1126/science.1214209.
Gillard, M., Leroy, S., Cannat, M., Sloan, H., 2021. Margin-to-margin seafloor spreading in the Eastern Gulf of Aden: a 16 ma-long history of deformation and magmatism from seismic reflection, gravity and magnetic data. Front. Earth Sci. 9, 707721 https://doi.org/10.3389/feart.2021.707721.
Girdler, R.W., Fairhead, J.D., Searle, R.C., Sowerbutts, W.T.C., 1969. Evolution of rifting in Africa. Nature 224, 1178–1182.
Grommé, C.S., Reilly, T.A., Mussett, A.E., Hay, R.L., 1970. Palaeomagnetism and Potassium-Argon ages of volcanic rocks of Ngorongoro Caldera, Tanzania. Geophys. J. R. Astron. Soc. 22, 101–105.
Guiraud, R., Bosworth, W., 1997. Senonian basin inversion and rejuvenation of rifting in Africa and Arabia: synthesis and implications to plate-scale tectonics. Tectonophysics 282, 39–82.
Guiraud, R., Maurin, J.-C., 1992. Early Cretaceous rifts of Western and Central Africa: an overview. Tectonophysics 213, 153–168.
Haileab, B., Brown, F.H., McDougall, I., Gathogo, P.N., 2004. Gombe Group basalts and initiation of Pliocene deposition in the Turkana depression, northern Kenya and southern Ethiopia. Geol. Mag. 141, 41–53. https://doi.org/10.1017/S001675680300815X.
Hajash, A., Armstrong, R.L., 1972. Paleomagnetic and radiometric evidence for the age of the Comores Islands, west central Indian Ocean. Earth Planet. Sci. Lett. 16, 231–236.
Halldórsson, S.A., Hilton, D.R.P.S., Abebe, T., Hopp, J., 2014. A common mantle plume source beneath the entire East African Rift System revealed by coupled helium-neon systematics. Geophys. Res. Lett. 41, 2304–2311. https://doi.org/10.1002/2014GL059424.
Hansen, S.E., Nyblade, A.A., Benoit, M.H., 2012. Mantle structure beneath Africa and Arabia from adaptively parameterized P-wave tomography: Implications for the origin of Cenozoic Afro-Arabian tectonism. Earth Planet. Sci. Lett. 319–320, 23–34. https://doi.org/10.1016/j.epsl.2011.12.023.
Hart, W.K., WoldeGabriel, G., Walter, R.C., Mertzman, S.A., 1989. Basaltic volcanism in Ethiopia: Constraints on continental rifting and mantle interactions. J. Geophys. Res. Solid Earth 94, 7731–7748. https://doi.org/10.1029/JB094iB06p07731.
Hartnady, C.J.H., 1990. Seismicity and plate boundary evolution in southeastern Africa. South Afr. J. Geol. 93, 473–484.
Hempton, M.R., 1987. Constraints on Arabian plate motion and extensional history of the Red Sea. Tectonics 6, 687–705.
Hill, R.I., 1991. Starting plumes and continental break-up. Earth Planet. Sci. Lett. 104, 398–416.
Hofmann, C., Courtillot, V., Feraud, G., Rochette, P., Yirgu, G., Ketefo, E., Pik, R., 1997. Timing of the Ethiopian flood basalt event and implications for plume birth and global change. Nature 389, 838–841.
Horner-Johnson, B.C., Gordon, R.G., Argus, D.F., 2007. Plate kinematic evidence for the existence of a distinct plate between the Nubian and Somalian plates along the Southwest Indian Ridge. J. Geophys. Res. 112, B05418. https://doi.org/10.1029/2006JB004519.
Iaffaldano, G., Davies, D.R., DeMets, C., 2018. Indian Ocean floor deformation induced by the Reunion plume rather than the Tibetan Plateau. Nature Geosc. 11, 362–366. https://doi.org/10.1038/s41561-018-0110-z.
Ishii, M., Tromp, J., 1999. Normal-mode and free-air gravity constraints on lateral variations in velocity and density of Earth's mantle. Science 285, 1231–1236. https://doi.org/10.1126/science.285.5431.1231.
Itaya, T., Sawada, Y., 1987. K-Ar ages of volcanic rocks in the Samburu hills area, northern Kenya. Afr. Study Monographs, Suppl. Issue 5, 27–45.
Jestin, F., Huchon, P., Gaulier, J.M., 1994. The Somalia plate and the East African Rift System: present-day kinematics. Geophys. J. Int. 116, 637–654.
Jolivet, L., Faccenna, C., 2000. Mediterranean extension and the Africa-Eurasia collision. Tectonics 19, 1095–1106.
Kampunzu, A.B., Mohr, P., 1991. Magmatic evolution and petrogenesis in the East African Rift System. In: Kampunzu, A.B., Lubala, R.T. (Eds.), Magmatism in Extensional Structural Settings. Springer-Verlag, Berlin, pp. 85–136.
Kendall, J.M., Lithgow-Bertelloni, C., 2016. Why is Africa Rifting? Geol. Soc. Lond., Spec. Publ. 420, 11–30. https://doi.org/10.1144/SP420.17.
Kent, P.E., Hunt, J.A., Johnstone, D.W., 1971. The Geology and Geophysics of Coastal Tanzania. Inst. Geol. Sci., London, Geophys. Paper, No, p. 6.
Kieffer, B., Arndt, N., Lapierre, H., Bastien, F., Bosch, D., Pecher, A., Yirgu, G., Ayalew, D., Weis, D., Jerram, D.A., Keller, F., Meugniot, C., 2004. Flood and Shield Basalts from Ethiopia: Magmas from the African Superswell. J. Petrol. 45, 793–834. https://doi.org/10.1093/petrology/egg112.
Kinabo, B.D., Atekwana, E.A., Hogan, J.P., Modisi, M.P., Wheaton, D.D., Kampunzu, A. B., 2007. Early structural development of the Okavango rift zone, NW Botswana. J. Afr. Earth Sci. 48, 125–136. https://doi.org/10.1016/j.jafrearsci.2007.02.005.
King, S.D., Ritsema, J., 2000. African hot spot volcanism: small-scale convection in the Upper Mantle Beneath Cratons. Science 290, 1137–1140.
Koptev, A., Calais, E., Burov, E., Leroy, S., Gerya, T., 2015. Dual continental rift systems generated by plume–lithosphere interaction. Nat. Geosci. 8, 388–392. https://doi.org/10.1038/ngeo2401.
Kuiper, K.F., Deino, A., Hilgen, F.J., Krijgsman, W., Renne, P.R., Wijbrans, J.R., 2008. Synchronizing rock clocks of Earth history. Science 320, 500–504.
Kusky, T.M., Toraman, E., Raharimahefa, T., Rasoazanamparany, C., 2010. Active tectonics of the Alaotra–Ankay Graben System, Madagascar: possible extension of Somalian–African diffusive plate boundary? Gondwana Res. 18, 274–294. https://doi.org/10.1016/j.gr.2010.02.003.
Laville, E., Piqué, A., Plaziat, J.-C., Gioan, P., Rakotomalala, R., Ravololonirina, Y., Tidahy, E., 1998. Le fossé méridien d'Ankay-Alaotra, témoin d'une extension crustale récente et actuelle à Madagascar. Bull. Soc. Géol. Fr. 169, 775–788.
Lemoine, A., Briole, P., Bertil, D., Roullé, A., Foumelis, M., Thinon, I., Raucoules, D., de Michele, M., Valty, P., Hoste Colomer, R., 2020. The 2018–2019 seismo-volcanic crisis east of Mayotte, Comoros islands: seismicity and ground deformation markers of an exceptional submarine eruption. Geophys. J. Int. 223, 22–44. https://doi.org/10.1093/gji/ggaa273.
Maccaferri, F., Rivalta, E., Keir, D., Acocella, V., 2014. Off-rift volcanism in rift zones determined by crustal unloading. Nat. Geosci. 7, 297–300. https://doi.org/10.1038/ngeo2110.
Macgregor, D., 2015. History of the development of the East African Rift System: a series of interpreted maps through time. J. Afr. Earth Sci. 101, 232–252. https://doi.org/10.1016/j.jafrearsci.2014.09.016.
Macgregor, D., 2018. History of the development of Permian. Pet. Geosci. 24, 8–20. https://doi.org/10.6084/m9.figshare.c.3902653.
Mao, W.L., Mao, H., Sturhahn, W., Zhao, J., Prakapenka, V.B., Meng, Y., Shu, J., Fei, Y., Hemley, R.J., 2006. Iron-rich post-perovskite and the origin of ultralow-velocity zones. Science 312, 564–565.
Mazzeo, F.C., Rocco, I., Tucker, R.D., D'Antonio, M., Melluso, L., 2021. Olivine melilitites, mantle xenoliths, and xenocrysts of the Takarindiona district: petrogenesis, magmatic evolution, and the sub-continental lithospheric mantle of east-central Madagascar. J. Afr. Earth Sci. 174, 104059.
McCartney, T., Scholz, C.A., 2016. A 1.3 million year record of synchronous faulting in the hangingwall and border fault of a half-graben in the Malawi (Nyasa) Rift. J. Struct. Geol. 91, 114–129. https://doi.org/10.1016/j.jsg.2016.08.012.
McDougall, I., Brown, F.H., 2008. Geochronology of the pre-KBS Tuff sequence, Omo Group, Turkana Basin. J. Geol. Soc. 165, 549–562.
McDougall, I., Brown, F.H., 2009. Timing of volcanism and evolution of the northern Kenya Rift. Geol. Mag. 146, 34–47. https://doi.org/10.1017/S0016756808005347.
McDougall, I., Feibel, C.S., 1999. Numerical age control for the Miocene–Pliocene succession at Lothagam, a hominoid-bearing sequence in the northern Kenya Rift. J. Geol. Soc. 156, 731–745.
McDougall, I., Watkins, R.T., 1988. Potassium-argon ages of volcanic rocks from northeast of Lake Turkana, northern Kenya. Geol. Mag. 125, 15–23.
McDougall, I., Watkins, R.T., 2006. Geochronology of the Nabwal Hills: a record of earliest magmatism in the northern Kenyan Rift Valley. Geol. Mag. 143, 25–39. https://doi.org/10.1017/S0016756805001184.
Melluso, L., Tucker, R.D., Cucciniello, C., le Roex, A.P., Morra, V., Zanetti, A., Rakotoson, R.L., 2018. The magmatic evolution and genesis of the Quaternary basanite-trachyphonolite suite of Itasy (Madagascar) as inferred by the geochemistry, Sr-Nd-Pb isotopes and trace element distribution in coexisting phases. Lithos 310-311, 50–64. https://doi.org/10.1016/j.lithos.2018.04.003.
Merkouriev, S., DeMets, C., 2006. Constraints on Indian plate motion since 20 Ma from dense Russian magnetic data: Implications for Indian plate dynamics. Geochem. Geophys. Geosyst. 7, 1–25. https://doi.org/10.1029/2005GC001079.
Meshesha, D., Shinjo, R., 2008. Rethinking geochemical feature of the Afar and Kenya mantle plumes and geodynamic implications. J. Geophys. Res. 113, B09209 https://doi.org/10.1029/2007JB005549.
Michon, L., 2016. The volcanism of the Comores archipelago integrated at a regional scale. In: Bachèlery, P., Lénat, J.-F., Di Muro, A., Michon, L. (Eds.), Active Volcanoes of the Southwest Indian Ocean Piton de la Fournaise and Karthala. Springer-Verlag, Berlin and Heidelberg, pp. 333–344.
Min, G., Hou, G., 2018. Geodynamics of the East African Rift System ~30 Ma ago: a stress field model. J. Geod. 117, 1–11. https://doi.org/10.1016/j.jog.2018.02.004.
Modisi, M.P., Atekwana, E.A., Kampunzu, A.B., Ngwisanyi, T.H., 2000. Rift kinematics during the incipient stages of continental extension: evidence from the nascent Okavango rift basin, northwest Botswana. Geology 28, 939–942.
Mohr, P, 1983. Ethiopian flood basalt province. Nature 303, 577–584.
Montagner, J.-P., Marty, B., Stutzmann, E., Sicilia, D., Cara, M., Pik, R., Lévêque, J.-J., Roult, G., Beucler, E., Debayle, E., 2007. Mantle upwellings and convective instabilities revealed by seismic tomography and helium isotope geochemistry beneath eastern Africa. Geophys. Res. Lett. 34, L21303. https://doi.org/10.1029/2007GL031098.
Montelli, R., Nolet, G., Dahlen, F.A., Masters, G., 2006. A catalogue of deep mantle plumes: new results from finite-frequency tomography. Geochem. Geophys. Geosyst. 7, Q11007. https://doi.org/10.1029/2006GC001248.
Morgan, W., 1971. Convection plumes in the lower mantle. Nature 230, 42–43.
Morley, C.K., 1988. Variable extension in Lake Tanganyika. Tectonics 7, 785–801.

Morley, C.K., Wescott, W.A., Stone, D.M., Harper, R.M., Wigger, S.T., Karanja, F.M., 1992. Tectonic evolution of the northern Kenyan Rift. J. Geol. Soc. 149, 333–348.
Morley, C.K., Ngenoh, D.K., Ego, J.K., 1999a. Introduction to the East African Rift System. In: Morley, C.K. (Ed.), Geoscience of Rift Systems—Evolution of East Africa. AAPG Studies in Geology, vol. 44, pp. 1–18.
Morley, C.K., Wescott, W.A., Stone, D.M., Harper, R.M., Wigger, S.T., Day, R.A., Karanja, F.M., 1999b. Geology and geophysics of the western Turkana basins, Kenya, in C.K. Morley ed., Geoscience of Rift Systems—Evolution of East Africa. AAPG Stud. Geol. 44, 19–54.
Mougenot, D., Recq, M., Virlogeux, P., Lepvrier, C., 1986. Seaward extension of the East African Rift. Nature 321, 599–603.
Mougenot, D., Hernandez, J., Virlogeux, P., 1989. Structure et volcanisme d'un rift sous-marin: le fossé des Kérimbas (marge nord-mozambique). Bull. Soc. Géol. Fr. 5, 401–410.
O'Connor, J.M., Jokat, W., Regelous, M., Kuiper, K.F., Miggins, D.P., Koppers, A.A.P., 2019. Superplume mantle tracked isotopically the length of Africa from the Indian Ocean to the Red Sea. Nat. Commun. 1–13 https://doi.org/10.1038/s41467-019-13181-7.
O'Connor, J., Jokat, W., Wijbrans, J., Colli, L., 2018. Hotspot tracks in the South Atlantic located above bands of fast flowing asthenosphere driven by waning pulsations from the African LLSVP. Gondwana Res. 53, 197–208. https://doi.org/10.1016/j.gr.2017.05.014.
Oxburgh, E.R., Turcotte, D., 1974. Menbrane tectonics and the East African Rift. Earth Planet. Sci. Lett. 22, 133–140.
Pastier, A.-M., Dauteuil, O., Murray-Hudson, M., Moreau, F., Walpersdorf, A., Makati, K., 2017. Is the Okavango Delta the terminus of the East African Rift System? Towards a new geodynamic model: Geodetic study and geophysical review. Tectonophysics 712-713, 469–481. https://doi.org/10.1016/j.tecto.2017.05.035.
Pelleter, A.-A., Caroff, M., Cordier, C., Bachèlery, P., Nehlig, P., Debeuf, D., Arnaud, N., 2014. Melilite-bearing lavas in Mayotte (France): an insight into the mantle source below the Comores. Lithos 208-209, 281–297. https://doi.org/10.1016/j.lithos.2014.09.012.
Phethean, J.J.J., Kalnins, L.M., van Hunen, J., Biffi, P.G., Davies, R.J., McCaffrey, K.J.W., 2016. Madagascar's escape from Africa: A high-resolution plate reconstruction for the Western Somali Basin and implications for supercontinent dispersal. Geochem. Geophys. Geosyst. 17, 5036–5055. https://doi.org/10.1002/2016GC006624.
Philippon, M., Corti, G., Sani, F., Bonini, M., Balestrieri, M.L., Molin, P., Willingshofer, E., Sokoutis, D., Cloetingh, S., 2014. Evolution, distribution and characteristics of rifting in the southern Ethiopia. Tectonics 33, 485–508. https://doi.org/10.1002/(ISSN)1944-9194.
Pickford, M.H., 1994. Patterns of sedimentation and fossil distribution in the Kenya Rift Valleys. J. Afr. Earth Sci. 18, 51–60.
Pik, R., Marty, B., Carignan, J., Lavé, J., 2003. Stability of the Upper Nile drainage network (Ethiopia) deduced from (U–Th)/He thermochronometry: implications for uplift and erosion of the Afar plume dome. Earth Planet. Sci. Lett. 215, 73–88. https://doi.org/10.1016/S0012-821X(03)00457-6.
Pik, R., Marty, B., Hilton, D.R., 2006. How many mantle plumes in Africa? The geochemical point of view. Chem. Geol. 226, 100–114. https://doi.org/10.1016/j.chemgeo.2005.09.016.
Pik, R., Marty, B., Carignan, J., Yirgu, G., Ayalew, T., 2008. Timing of East African Rift development in southern Ethiopia: Implication for mantle plume activity and evolution of topography. Geology 36, 167–170. https://doi.org/10.1130/G24233A.1.
Piqué, A., Laville, E., Chotin, P., Chorowicz, J., Rakotondraompiana, S., Thouin, C., 1999. Neogene and present extension in Madagascar: structural and geophysical data. J. Afr. Earth Sci. 28, 975–983.
Ponte, J.-P., Robin, C., Guillocheau, F., Popescu, S., Suc, J.-P., Dall'Asta, M., Melinte-Dobrinescu, M.C., Bubik, M., Dupont, G., Gaillot, J., 2019. The Zambezi delta (Mozambique channel, East Africa): High resolution dating combining bio- orbital and seismic stratigraphies to determine climate (palaeoprecipitation) and tectonic controls on a passive margin. Mar. Pet. Geol. 105, 293–312. https://doi.org/10.1016/j.marpetgeo.2018.07.017.
Presnall, D.C., Gudfinnsson, G.H., 2005. Carbonate-rich melts in the oceanic low-velocity zone and deep mantle. In: Foulger, G.R., Natland, J.H., Presnall, D.C., Anderson, D.L. (Eds.), Plates, Plumes and Paradigms, Geological Society of America Special Paper. American Geophysical Union, pp. 207–216.
Ritsema, J., Van Heijst, H.J., Woodhouse, J.H., 1999. Complex shear wave velocity structure imaged beneath Africa and Iceland. Science 286, 1925–1928.
Ritsema, J., Deuss, A., van Heijst, H.J., Woodhouse, J.H., 2010. S40RTS: a degree-40 shear-velocity model for the mantle from new Rayleigh wave dispersion, teleseismic traveltime and normal-mode splitting function measurements. Geophys. J. Int. 184, 1223–1236. https://doi.org/10.1111/j.1365-246X.2010.04884.x.
Roberts, E.M., O'Connor, P.M., Stevens, N.J., Gottfried, M.D., Jinnah, Z.A., Ngasala, S., Choh, A.M., Armstrong, R.A., 2010. Sedimentology and depositional environments of the Red Sandstone Group, Rukwa Rift Basin, southwestern Tanzania: New insight into Cretaceous and Paleogene terrestrial ecosystems and tectonics in sub-equatorial Africa. J. Afr. Earth Sci. 57, 179–212. https://doi.org/10.1016/j.jafrearsci.2009.09.002.
Roberts, G.G., Paul, J.D., White, N., Winterbourne, J., 2012a. Temporal and spatial evolution of dynamic support from river profiles: a framework for Madagascar. Geochem. Geophys. Geosyst. 13, Q04004. https://doi.org/10.1029/2012GC004040.
Roberts, E.M., Stevens, N.J., O'Connor, P.M., Dirks, P.H.G.M., Gottfried, M.D., Clyde, W. C., et al., 2012b. Initiation of the western branch of the East African Rift coeval with the eastern branch. Nature Geosc. 5, 289–294. https://doi.org/10.1038/ngeo1432.
Rogers, N., Macdonald, R., Fitton, J.G., George, R., Smith, M., Barreiro, B., 2000. Two mantle plumes beneath the East African rift system: Sr, Nd and Pb isotope evidence from Kenya Rift basalts. Earth Planet. Sci. Lett. 176, 387–400.
Rooney, T.O., Herzberg, C., Bastow, I.D., 2012. Elevated mantle temperature beneath East Africa. Geology 40, 27–30.
Rooney, T.O., Nelson, W.R., Furman, T., Hanan, B.B., 2014. The role of continental lithosphere metasomes in the production of HIMU-like magmatism on the northeast African and Arabian plates. Geology 42, 419–422.
Rosendahl, B.R., 1987. Architecture of continental rifts with special reference to East Africa. Annu. Rev. Earth Planet. Sci. 15, 445–503.
Rudnick, R.L., McDonough, W.F., Chappell, B.W., 1993. Carbonatite metasomtism in the northern Tanzanian mantle: petrographic and geochemical characteristics. Earth Planet. Sci. Lett. 114, 463–475.
Rufer, D., Preusser, F., Schreurs, G., Gnos, E., Berger, A., 2014. Late Quaternary history of the Vakinankaratra volcanic field (central Madagascar): insights from luminescence dating of phreatomagmatic eruption deposits. Bull. Volcanol. 76, 817 https://doi.org/10.1007/s00445-014-0817-7.
Ruppel, C., 1995. Extensional processes in continental lithosphere. J. Geophys. Res. 100, 24187–24215.
Sawada, Y., Tateishi, M., Ishida, S., 1987. Geology of the Neogene system in and around the Samburu hills, Northern Kenya. Afr. Study Monographs, Suppl. Issue, vol. 5, pp. 7–26.
Sengör, A.M.C., Burke, K., 1978. Relative timing of rifting and volcanism on Earth and its tectonic implications. Geophys. Res. Lett. 5, 419–421.
Shackleton, R.M., 1996. The final collision zone between East and West Gondwana: where is it? J. Afr. Earth Sci. 23, 271–287.
Simmons, N.A., Forte, A.M., Boschi, L., Grand, S.P., 2010. GyPSuM: a joint tomographic model of mantle density and seismic wave speeds. J. Geophys. Res. 115, B12310 https://doi.org/10.1029/2010JB007631.
Simon, B., Guillocheau, F., Robin, C., Dauteuil, O., Nalpas, T., Pickford, M., et al., 2017. Deformation and sedimentary evolution of the Lake Albert Rift (Uganda, East African Rift System). Mar. Pet. Geol. 86, 17–37. https://doi.org/10.1016/j.marpetgeo.2017.05.006.
Smith, I.E.M., Brenna, M., Cronin, S.J., 2021. The magma source of small-scale intraplate monogenetic volcanic systems in northern New Zealand. J. Volcanol. Geotherm. Res. 418, 107326 https://doi.org/10.1016/j.jvolgeores.2021.107326.
Späth, A., le Roex, A.P., Duncan, R.A., 1996. The Geochemistry of Lavas from the Comores Archipelago, Western Indian Ocean: Petrogenesis and Mantle Source Region Characteristics. J. Petrol. 37, 961–991.
Spera, F.J., Fowler, S.J., 2009. Conceptual model for small-volume alkali basalt petrogenesis: implications for volcanic hazards at the proposed Yucca Mountain nuclear waste repository. In: Connor, C., Connor, L., Chap-man, N. (Eds.), Volcanism, Tectonism, and Siting Nuclear Facilities. Cambridge University Press, Cambridge, UK, pp. 195–228.
Spiegel, C., Kohn, B.P., Belton, D.X., Gleadow, A.J.W., 2007. Morphotectonic evolution of the central Kenya rift flanks: Implications for late Cenozoic environmental change in East Africa. Geology 35, 427–430. https://doi.org/10.1130/G23108A.1.
Stab, M., Bellahsen, N., Pik, R., Quidelleur, X., Ayalew, D., Leroy, S., 2016. Modes of rifting in magma-rich settings: Tectono-magmatic evolution of Central Afar. Tectonics 35, 2–38. https://doi.org/10.1002/(ISSN)1944-9194.
Stamps, D.S., Iaffaldano, G., Calais, E., 2015. Role of mantle flow in Nubia-Somalia plate divergence. Geophys. Res. Lett. 42, 290–296. https://doi.org/10.1002/(ISSN)1944-8007.
Stamps, D.S., Saria, E., Kreemer, C., 2018. A geodetic strain rate model for the East African Rift System. Sci. Rep. 8, 732. https://doi.org/10.1038/s41598-017-19097-w.
Stamps, D.S., Kreemer, C., Fernandes, R., Rajaonarison, T.A., Rambolamanana, G., 2021. Redefining East African Rift System kinematics. Geology 49 (2), 150–155. https://doi.org/10.1130/G47985.1.
Suwa, G., White, T., Asfaw, B., WoldeGabriel, G., Yemane, T., 1991. Miocene faunal remains from the Burji-Soyama area, Amaro horst, southern sector of the Main Ethiopian Rift. Palaeontol. Afr. 28, 23–28.
Tatsumi, Y., Kimura, N., 1991. Secular variation of basalt chemistry in the Kenya Rift: evidence for the pulsing of asthenospheric upwelling. Earth Planet. Sci. Lett. 104, 99–113.
Thorpe, R.S., Smith, K., 1974. Distribution of Cenozoic volcanism in Africa. Earth Planet. Sci. Lett. 22, 91–95. https://doi.org/10.1016/0012-821X(74)90068-5.
Torres Acosta, V., Bande, A., Sobel, E.R., Parra, M., Schildgen, T.F., Stuart, F., Strecker, M.R., 2015. Cenozoic extension in the Kenya Rift from low-temperature thermochronology: Links to diachronous spatiotemporal evolution of rifting in East Africa. Tectonics 34, 2367–2386.
Torsvik, T.H., Smethurst, M.A., Burke, K., Steinberger, B., 2006. Large igneous provinces generated from the margins of the large low-velocity provinces in the deep mantle. Geophys. J. Int. 167, 1447–1460. https://doi.org/10.1111/j.1365-246X.2006.03158.x.
Trampert, J., Deschamps, F., Resovsky, J., Yuen, D., 2004. Probabilistic tomography maps chemical heterogeneities throughout the lower mantle. Science 306, 853–856.
Tsekhmistrenko, M., Sigloch, K., Hosseini, K., Barruol, G., 2021. A tree of Indo-African mantle plumes imaged by seismic tomography. Nat. Geosci. 14, 612–619. https://doi.org/10.1038/s41561-021-00762-9.
Ukstins, I.A., Renne, P.R., Wolfenden, E., Baker, J., Ayalew, D., Menzies, M., 2002. Matching conjugate volcanic rifted margins: 40AR/39Ar chrono-stratigraphy of pre- and syn-rift bimodal flood volcanism in Ethiopia and Yemen. Earth Planet. Sci. Lett. 198, 289–306.

Valentine, G.A., Hirano, N., 2010. Mechanisms of low-flux intraplate volcanic fields—Basin and Range (North America) and northwest Pacific Ocean. Geology 38, 55–58. https://doi.org/10.1130/G30427.1.

Valentine, G.A., Perry, F.V., 2007. Tectonically controlled, time-predictable basaltic volcanism from a lithospheric mantle source (central Basin and Range Province, USA). Earth Planet. Sci. Lett. 261, 201–216. https://doi.org/10.1016/j.epsl.2007.06.029.

Vérard, C., 2021. 888-444 Ma global plate tectonic reconstruction with emphasis on the formation of Gondwana. Front. Earth Sci. 9, 666153 https://doi.org/10.3389/feart.2021.666153.

Wang, S., Yu, H., Zhang, Q., Zhao, Y., 2018. Absolute plate motions relative to deep mantle plumes. Earth Planet. Sci. Lett. 490, 88–99. https://doi.org/10.1016/j.epsl.2018.03.021.

Wessa, P., 2015. Kernel Density Estimation (v1.0.12) in Free Statistics Software (v1.2.1), Office for Research Development and Education, URL. http://www.wessa.net/rwasp_density.wasp/.

Wichura, H., Bousquet, R., Oberhansli, R., Strecker, M.R., Trauth, M.H., 2010. Evidence for middle Miocene uplift of the East African Plateau. Geology 38, 543–546. https://doi.org/10.1130/G31022.1.

Williams, L.A.J., 1982. Physical Aspects of Magmatism in Continental Rifts. In: Continental and Oceanic Rifts, G. Pálmason (Ed.) 8, 193–222. https://doi.org/10.1029/GD008p0193.

Wilson, M., Guiraud, R., 1992. Magmatism and rifting in Western and Central Africa, from Late Jurassic to Recent times. Tectonophysics 213, 203–225.

WoldeGabriel, G., Aronson, J.L., Walter, R.C., 1990. Geology, geochronology, and rift basin development in the central sector of the Main Ethiopia Rift. Geol. Soc. Am. Bull. 102, 439–458.

Wolfenden, E., Ebinger, C., Yirgu, G., Deino, A., Ayalew, D., 2004. Evolution of the northern Main Ethiopian rift: birth of a triple junction. Earth Planet. Sci. Lett. 224, 213–228. https://doi.org/10.1016/j.epsl.2004.04.022.

Wolfenden, E., Ebinger, C., Yirgu, G., Renne, P.R., Kelley, S.P., 2005. Evolution of a volcanic rifted margin: Southern Red Sea, Ethiopia. Geol. Soc. Am. Bull. 117, 846–864. https://doi.org/10.1130/B25516.1.

Wooley, A.R., 2001. Alkaline Rocks and Carbonatites of the World. Part 3: Africa. The Geological Society of London, London.